



Cite this: *Nanoscale Horiz.*, 2025,  
10, 258

## “Sweet MOFs”: exploring the potential and restraints of integrating carbohydrates with metal–organic frameworks for biomedical applications

Alessio Zuliani, <sup>a</sup> Victor Ramos, <sup>a</sup> Alberto Escudero <sup>ab</sup> and Noureddine Khiar <sup>\*a</sup>

The unique features of metal–organic frameworks (MOFs) such as biodegradability, reduced toxicity and high surface area offer the possibility of developing smart nanosystems for biomedical applications through the simultaneous functionalization of their structure with biologically relevant ligands and the loading of biologically active cargos, ranging from small drugs to large biomacromolecules, into their pores. Aiming to develop efficient, naturally inspired biocompatible systems, recent research has combined organic and materials chemistry to design innovative composites that exploit carbohydrate chemistry for the functionalization and structural modification of MOFs. Scientific investigation in the field has seen a significant rise in the past five years, and it is becoming crucial to acknowledge both the limits and benefits of this approach for future investigation. In this review, the latest research results merging carbohydrates and MOFs are discussed, with a particular emphasis on the advances in the field and the remaining challenges, including addressing sustainability and real-case applicability.

Received 15th October 2024,  
Accepted 1st November 2024

DOI: 10.1039/d4nh00525b

rsc.li/nanoscale-horizons

### Introduction

Carbohydrates (CHs), fundamental building blocks of life alongside lipids, proteins, and nucleic acids, have long captivated researchers with their diverse structure and biological functionalities. Beyond their crucial role in biological signalling, CHs exhibit a myriad of other biological functions, including energy storage, organelle protection, modulation of peptide or protein properties, mediating cellular and extracellular interactions, but also immune response, inflammation and tumor cell metastasis.<sup>1</sup> Besides, different CHs mediate interactions with pathogens during the early and crucial stages of infection, as happens with the adherent-invasive and uropathogenic (UPEC) *Escherichia coli*, HIV-1 virus, influenza, Ebola and coronavirus.<sup>2</sup> For example, it has been demonstrated that the entry of SARS-CoV2 pseudo-typed virus into cells can significantly be inhibited by heparin.<sup>3</sup> CHs are also involved in bacterial infection processes. This is the case for *Pseudomonas aeruginosa*, a bacterium that is a leading cause of morbidity and mortality in cystic fibrosis patients and immunocompromised

individuals, which specifically targets galactose and strongly binds to fucose and fucose-containing oligosaccharides to adhere to epithelial cells.

These essential biological interactions, combined with their biocompatibility and biodegradability, make CHs ideal for a wide range of biomedical applications, spanning from glyco-based drugs,<sup>4,5</sup> drug delivery, diagnosis, and imaging to tissue engineering, wound healing, and antiviral/antimicrobial treatments.<sup>6–10</sup> Nevertheless, the direct use of CHs in biomedical applications is often limited by their structural complexity, low affinity, poor stability, rapid degradation in the body, and lack of controlled release of eventually coupled drugs. Additionally, their solubility and targeting abilities can be suboptimal without further modification. As a result, during the last two decades, research has focused on the design of a variety of glyco-nanomaterials capable of addressing these intrinsic limitations of CHs, including hydrogels, nanotubes, liposomes, micelles, nanoparticles, dendrimers, and metal–organic frameworks (MOFs).<sup>11–20</sup> These CH-based nanosystems feature unique characteristics, such as high avidity coupled with specific recognition by various cell surface receptors, which significantly enhance the receptor-mediated uptake of nanocarriers, thanks also to the exploitation of multivalency, *i.e.*, the presence of multiple copies of the same element on the surface of each nanovector.<sup>21</sup> For example, surface modifications employing specific sugars, such as D-mannose, have been demonstrated to increase the receptor-

<sup>a</sup> Asymmetric Synthesis and Nanosystems Group (Art&Fun), Institute for Chemical Research (IIQ), CSIC-University of Seville, 41092 Seville, Spain.

E-mail: [khiar@iiq.csic.es](mailto:khiar@iiq.csic.es)

<sup>b</sup> Inorganic Chemistry Department, University of Seville, Calle Profesor García González 1, 41012 Seville, Spain



mediated uptake of nanocarriers of drugs,<sup>22</sup> whereas modifications with other saccharides, like dextrin (a glucose polysaccharide), can mitigate nonspecific cellular uptake.<sup>23</sup> Moreover, CH-based nanocarriers which are partially or entirely composed of saccharides, are susceptible to cellular degradation, leading to the subsequent release of the payload. This property is particularly beneficial for the clearance of these materials from the body and for triggering drug release or activation by specific enzymes. CHs can also be encapsulated inside specific nanostructures, in order to guarantee protection of the drug from enzymatic degradation, controlled release kinetics, targeted delivery to affected areas, and enhanced bioavailability.<sup>24</sup>

Among all, the combination of CHs with metal-organic frameworks (MOFs) has garnered significant interest based on the exploitation of their unique features including their ability to load different active molecules thanks to their adjustable porosity and pore sizes, and their variable composition that allows the incorporation of a variety of multivariate structures with single, double, or triple metal systems and/or organic linkers. Additionally, they can utilize flexible linkers and versatile inorganic building units in terms of geometry. Furthermore, MOFs can undergo post-synthetic modifications (PSM) to introduce new functional groups, which can be applied to both the external surfaces and internal pore structures.<sup>25–27</sup> Even though the first articles related to MOFs and CH-based nanosystems can be dated back to the early 2010s,<sup>28,29</sup> the flowering of this research area only began not long ago, starting around 2020. This recent blossoming initiated thanks to the improvements in the technologies and methodologies for the preparation of MOFs and in carbohydrate synthetic processes, as well as to the breakthroughs in immunotherapy, targeted treatments, nanomedicine, and personalized medicine.<sup>30–32</sup> Thus, this field of research is still in its infancy, although it is rapidly growing.

The nanostructures forged by the fusion of CHs and MOFs, which we have poetically defined as “Sweet” MOFs and referred from here on as “CHs-MOFs” for convenience and ease of reading, present a compelling opportunity in the field of biomedicine, as these systems merge the advantageous properties of both components. From a theoretical perspective, CHs-MOFs offer several unique features that distinguish them from other nanoparticles for biomedical applications including:

- Enhanced biocompatibility: CHs, as natural occurring chemicals, can improve the compatibility of MOFs within biological environments, reducing potential toxicity concerns commonly associated with synthetic materials. This biocompatibility is critical for applications such as drug delivery or tissue engineering, where the interaction of the material with the body must be benign and support cellular functions. Furthermore, the introduction of CHs with finely designed molecular structure can allow for the targeting of specific receptors. For example, sialic acids, particularly *N*-acetylneurameric acid (Neu5Ac), target Siglec receptors on immune cells to modulate immune responses, with applications in immune regulation and cancer immunotherapy.<sup>33</sup> Also, heparan sulfate, a highly sulfated glycosaminoglycan, has been studied for the potential targeting of heparan sulfate proteoglycan (HSPG) receptors on cells, with

applications in inhibiting viral entry and targeting angiogenesis in cancer therapy.<sup>34</sup>

- Porous structure: MOFs possess highly tuneable, porous frameworks that are ideal for encapsulating therapeutic agents. The porous nature protects the drug molecules from premature degradation and facilitates controlled release, which is essential for achieving sustained therapeutic effects. CHs can further assist in modulating this release profile, leveraging their responsiveness to biological cues such as enzymatic degradation or pH changes.<sup>35,36</sup>

- Modular nature: the combination of CHs and MOFs enables the design of nanosystems with customizable physico-chemical properties, including size, surface charge, and hydrophobicity. This tunability enhances the targeting specificity and therapeutic efficacy of drug delivery systems, offering opportunities for personalized medicine and treatments that demand high precision, such as in cancer or gene therapy.<sup>37,38</sup>

Nevertheless, despite the potential of CHs-MOFs, several substantial challenges remain: (I) scalability and reproducibility remain major concerns, as the synthesis of MOFs often relies on intricate protocols that may hinder large-scale production; (II) the sustainable features of these nanosystems are also a poorly explored theme, in contrast with recent trends and modern environmental policies; (III) ensuring the long-term stability of CHs-MOFs in complex biological environments poses a formidable obstacle, requiring meticulous optimization and characterization; (IV) elucidating and optimizing the intricate interplay between CHs and MOFs within biological systems is imperative to address their full therapeutic potential.

The current literature reports several relevant reviews on the exploitation of MOFs in biomedicine, spanning applications from drug delivery systems (DDSs) for cancer therapy and diagnostics (theragnostic) for antibacterial and wound healing systems.<sup>39–42</sup> For example, some studies focus on single and multiple stimuli-responsive DDSs, while others explore polymer/MOF hybrid systems and MOF-based DDSs for advanced drug delivery, emphasizing drug loading strategies, applications, biopharmaceutics, and quality control.<sup>37,38,42–44</sup> To the best of our knowledge, the only reviews relating to CHs and MOFs were specifically focused on cyclodextrin-based MOFs (CD-MOFs), including a review reported by Stoddart *et al.*,<sup>45</sup> another one by Huang *et al.*, who focused on biological MOFs made with different bioligands, including cyclodextrins,<sup>46</sup> and a recent review by Cha and collaborators.<sup>47</sup> A book chapter exploring the field of CD-MOFs is also available in the literature.<sup>26</sup> A review from 2020 explored the theme of CH-MOFs as part of the different bio entities coupled with MOFs.<sup>35</sup>

In contrast, this review aims at providing a general overview of the different classes of materials derived from the combination of CHs and MOFs, contributing to a concise summary of the current state-of-the-art research toward future developments. More in detail, this review delves into the exclusive characteristics and current limitations of the strategies for merging CH chemistry with MOFs for biomedical purposes, with a brief look at industrial interests and prospects. The title, “Sweet MOFs”, is a tribute to the etymology and ancient



## CHs-MOFs

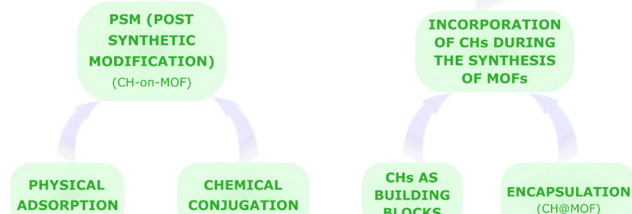


Fig. 1 Scheme of the most common strategies for the preparation of carbohydrate-MOFs (CHs-MOFs).

meaning of the term “saccharide”, from the Latin “*saccharum*”, defined as “...a kind of honey found in cane, white as gum, and it crunches between the teeth...” (Pliny the Elder), derived from the Ancient Greek word *σάκχαρον* (sakkharon).<sup>48</sup> The review firstly reports a brief discussion of the most studied CHs and MOFs for the preparation of CHs-MOFs. In particular, the biological role and uses of the CHs are summarised as well as the characteristics of the main classes of MOFs studied for biomedical applications. Then, the review is subdivided into two sections, one focused on the most recent strategies for the post synthetic modification (PSM) of MOFs with CHs, forming the so-defined CHs-on-MOFs,<sup>35</sup> and the other focusing on the incorporation of carbohydrates during the synthesis of MOFs, whether as part of the same structure as the MOF or encapsulated in it, *i.e.*, CHs@MOFs,<sup>35</sup> as summarised in Fig. 1. Finally, this review reports some selected examples of preclinical trials of CHs-MOFs, followed by an outlook and conclusion section.

## Most studied carbohydrates and MOFs for the development of CHs-MOFs

### Carbohydrates

Serving as a primary source of energy for living organisms and covering other biological functions ranging from cell signalling and cellular recognition to structural support to cells, CHs, herein referred as a synonym of saccharide,<sup>49</sup> encompass different classes of compounds, *i.e.*, simple monosaccharides, such as glucose and fructose, disaccharides, such as sucrose and lactose, oligosaccharides, containing a small number of sugar units (usually 3–10), and polysaccharides, such as starch, glycogen, and cellulose.

CHs are incorporated into CHs-MOFs to enhance various functional properties, including:

- Improved biocompatibility: for example, when CHs are used as building units in CHs-MOFs, their degradation products are non-toxic, minimizing concerns related to toxicity.
- Enhanced solubility and dispersibility: the hydrophilic nature of CHs boosts the aqueous solubility and colloidal stability of MOFs, improving their behaviour in biological systems.
- Enhanced avidity: to offset the intrinsically low affinity associated with monomeric carbohydrate–protein binding interactions.<sup>50</sup>
- Targeting capabilities: specific CHs can be designed to interact with cellular receptors, enabling targeted delivery of drugs or imaging agents to specific tissues or cell types.
- Controlled release of active compounds: CHs-MOFs can be engineered to regulate the release kinetics of encapsulated drugs or other active agents, ensuring sustained or stimuli-responsive delivery. For example, CHs can also function as “gatekeepers” by forming a film around drug-loaded MOFs,

Monosaccharides	Polysaccharides
<p>Glucose</p> <ul style="list-style-type: none"> <li>- Treat medical conditions</li> <li>- Mainly used in the food industry</li> <li>- Industrial production by hydrolysis of starch</li> </ul>	<p>Cyclodextrins</p> <ul style="list-style-type: none"> <li>- Ability to encapsulate hydrophobic substances</li> <li>- Pharmaceuticals, food industry and environmental applications</li> <li>- Industrial production by degradation of starch</li> </ul>
<p>Galactose</p> <ul style="list-style-type: none"> <li>- Affinity to receptors of various diseases, as hepatic cancer</li> <li>- Many industrial applications</li> <li>- Industrial production by hydrolysis of lactose</li> </ul>	<p>Chitosans</p> <ul style="list-style-type: none"> <li>- Antimicrobial, antioxidant and wound-healing properties</li> <li>- Pharmaceutical and food industry applications</li> <li>- Industrial production by deacetylation of chitin</li> </ul>
<p>Mannose</p> <ul style="list-style-type: none"> <li>- Many medical applications especially against cancer</li> <li>- Diverse industrial applications</li> <li>- Industrial production by extraction from plants</li> </ul>	<p>Glycosaminoglycans</p> <ul style="list-style-type: none"> <li>- Widely used in medicine</li> <li>- Pharmaceutic, cosmetic and nutraceutic ingredient</li> <li>- Industrial production by extraction from animals</li> </ul>

Fig. 2 Structures of the most studied carbohydrates for the preparation of CHs-MOFs.



controlling the release of the drugs as the film gradually degrades.<sup>51</sup>

Currently, the main CHs utilized for designing CHs-MOFs for biomedical applications encompass a wide array of compounds and their derivatives, such as chitosan, hyaluronic acid, dextran, cyclodextrins, glucose and galactose. Chitosan, derived from chitin, stands out for its biocompatibility and adhesive properties, finding utility in drug delivery, gene therapy, imaging, and tissue engineering.<sup>52</sup> Meanwhile, the compatibility and ability to target specific cancer cell receptors of hyaluronic acid (HA) make it valuable for targeted drug delivery and cancer imaging.<sup>53</sup> Dextran-coated MOFs offer versatility in drug delivery, imaging, and theragnostic applications, thanks to their biocompatibility and stealth properties.<sup>54</sup> Cyclodextrin-functionalized MOFs excel at encapsulating hydrophobic drugs, enhancing their solubility and stability.<sup>55</sup> Glucose-functionalized MOFs are engineered to precisely target cancer cells while minimizing off-target effects by leveraging glucose transporter overexpression.<sup>56</sup> Similarly, galactose-MOFs exhibit targeting capabilities for liver cells, promising advancements in liver-targeted drug delivery and imaging.<sup>57</sup> Fig. 2 summarises the main industrial uses as well as the principal large-scale production methods among the most studied CHs – and their derivatives – for the preparation of CHs-MOFs, including glucose, cyclodextrins (CD), chitosan, galactose, mannose, and glycosaminoglycans (GAGs).

## MOFs

Metal organic frameworks (MOFs), unique structures of metal-containing inorganic building units, *i.e.*, metal ions or metal clusters, connected to multidentate organic building units, *i.e.*, (organic) linkers, *via* coordination bonding, belong to the almost 30-year old class of reticular materials. MOFs exhibit highly adjustable physicochemical and structural properties, which in turn affect their functionality. One of the primary advantages of MOFs is their exceptionally high surface area and tuneable porosity, which allow for efficient drug loading and storage of therapeutic agents. This adjustable pore size can be precisely engineered to accommodate various drug molecules, enabling controlled release profiles that respond to specific physiological conditions. Additionally, their customizable multi-faceted structures with multiple metals (such as mono-, bi-, or tri-metallic systems) and/or organic linkers allows for the use of conformationally flexible linkers and/or geometrically adaptable inorganic building units as well as for functionalization with targeting ligands or biomolecules, enhancing specificity towards diseased tissues or cells, such as cancer.<sup>58</sup> Moreover, certain MOFs, such as those belonging to the class of “PCN” can be used for specific applications in photodynamic therapy (PDT) and photothermal therapy (PTT).

The myriad combinations of metal nodes and organic linkers offer an almost boundless array of possibilities for creating MOFs. However, even though the structures of MOFs reported to date exceed 100k units, only a limited number of MOF classes have been investigated for biomedical applications.<sup>59</sup> This limitation mainly arises from the complexities of the pharmacokinetics of MOFs, in terms of absorption, distribution, metabolism,

excretion, and toxicity (ADME-Tox or ADMET), which narrow down the pool of MOFs suitable for designing nanocarriers.<sup>60</sup> Unfortunately, a comprehensive understanding of the ADME-Tox of MOFs, remains elusive, leading to the selection of MOFs for biological applications based on rough and more general criteria. In this regard, a recent review delves deeply into the ADMET of nanoparticles in general, emphasizing the ongoing need for further investigation into this practically unknown area.<sup>61</sup> Currently, the types of MOFs used to prepare CHs-MOFs mainly belong to the UiO, ZIF, PCN, MIL, and CD-MOF families, whose key characteristics are summarized in Fig. 3.

## Designing CHs-MOFs

### Features

When designing MOFs-CHs, a sequence of characteristics should be considered, including biological compatibility, such as toxicity, biodegradability, and chemical stability, size- and shape-controlled synthesis, as well as surface and pore volume versatility.

- **Toxicity:** CHs-MOFs should exhibit low toxicity *per se*, and their degradation products, *i.e.*, the metal nodes and the organic components, should also be biocompatible. This implies the use of metals with low toxicity, such as those naturally occurring in the body like magnesium, calcium, and some d-block transition metals (*e.g.*, iron, cobalt, manganese, copper, zinc, molybdenum), as well as other metals known for their relatively low toxicity such as zirconium and titanium. Regarding the organic components, *i.e.*, the organic linkers and the CHs (as long as the CHs themselves do not serve as organic linkers), a variety of compounds ranging from fumaric acid and terephthalic acid to porphyrin-based linkers are commonly employed, alongside natural compounds like adenine, aspartate, or cyclodextrins. Importantly, the lethal dose 50 values ( $LD_{50}$ ) for these types of metal and ligands are substantially high (*i.e.* their toxicity is low). For example, the  $LD_{50}$  of Cu is  $25\text{ mg kg}^{-1}$ , that of terephthalic acid is  $5\text{ g kg}^{-1}$ , and that of  $\beta$ -CD is *ca.*  $18\text{ g kg}^{-1}$ . These values are even less impactful given the minimal amounts of metals and ligands required to prepare the few milligrams of CHs-MOFs used in biomedical applications.

- **Chemical stability and biodegradability:** CHs-MOFs should also show the right balance between being chemically stable and biodegradable. They should remain stable in biological fluids until they reach their target site but break down within a certain timeframe (few hours/days) to avoid accumulating in the body. The biodegradation can also happen in response to external triggers, like changes in pH or the presence of specific enzymes found in certain parts of the body, like certain types of tumours. Currently, researchers are running into more challenges with CHs-MOFs stability compared to their biodegradability. This is particularly evident when CHs-MOFs are exposed to solutions simulating the human body, such as phosphate solutions (*e.g.*, PBS, pH 7.4) or artificial lysosomal fluid (ALF, pH 4.4). The stability in PBS is particularly challenging since phosphate ions have good affinity towards some metal ions/clusters, thus they tend to replace the organic ligands. To tackle this,



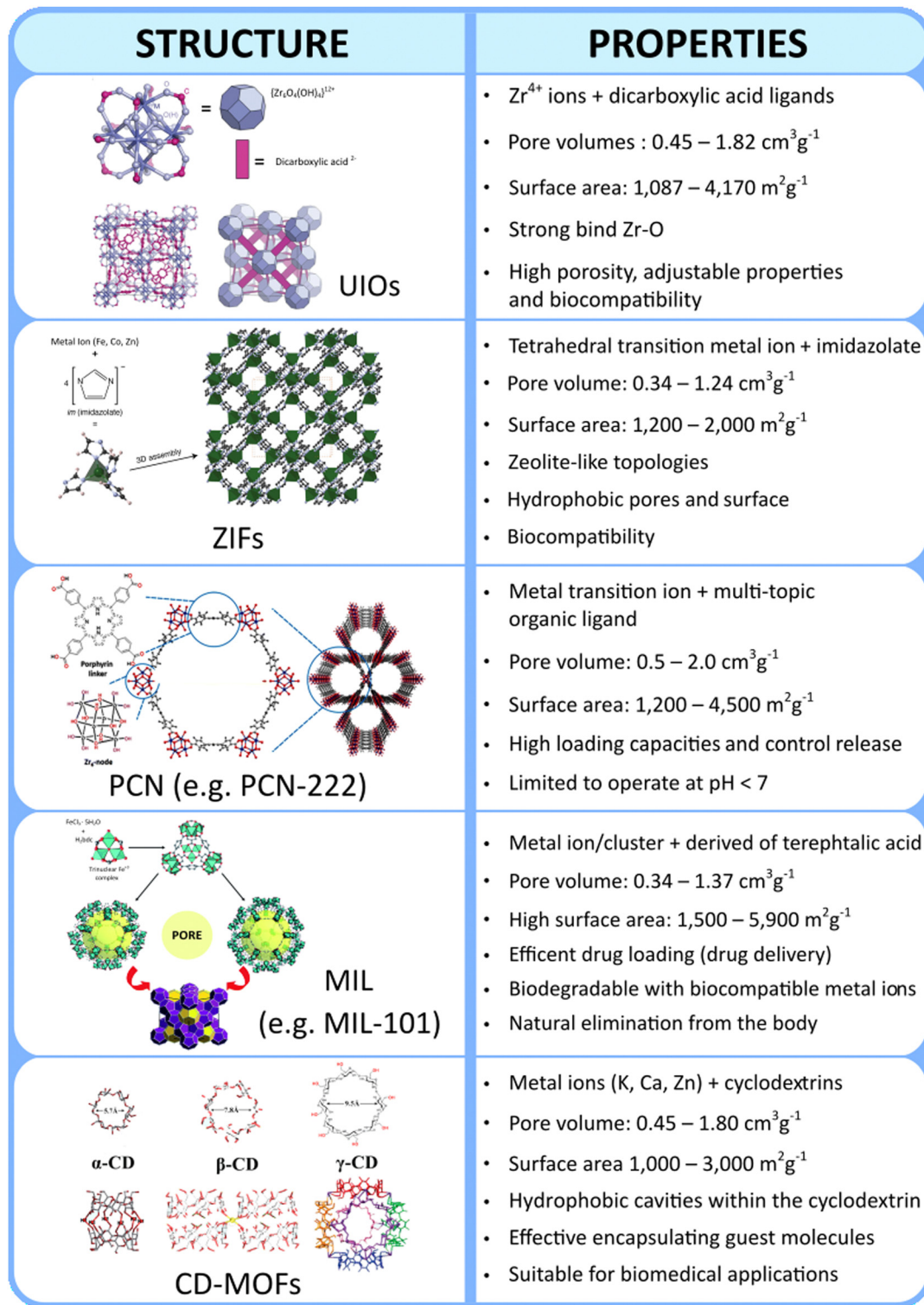


Fig. 3 Structures and relevant features of the most studied MOFs for the preparation of CHs-MOFs.

some approaches involve the introduction of structural defects with specific organic compounds, such as in the case of the utilization of amino terephthalic acids in UiO-66, or coating MOFs with long-chain molecules like poly ethylene glycols (PEGs) or polysaccharides.

- Shape and size: when discussing the shape and size of nanoparticles for biomedical applications, which are crucial for the circulation in the body and ability to penetrate cells, especially for targeting applications, the literature offers a complex range of perspectives and sometimes conflicting



opinions regarding the ideal nanocarrier. A point of agreement is that particles with a hydrodynamic diameter (HD) smaller than 5.5 nm are swiftly eliminated *via* urinary excretion and particles should ideally be smaller than 200 nm to evade detection by the mononuclear phagocyte system. Therefore, nanosystems for biomedical applications should ideally fall within a hydrodynamic (HD) size range of 5.5–200 nm, ensuring that any potential agglomerates do not obstruct the smallest blood vessels in the body, *i.e.*, the capillaries. In alignment with the current literature, the majority of CHs-MOFs are indeed prepared with sizes below 200 nm. However, investigations into how the shapes and sizes of CHs-MOFs influence their dynamics in bodily fluids and, more generally, their ADMET profile are rarely conducted. Consequently, the selection of shape and size is primarily based on reported literature, even when referring to other types of MOFs or nanoparticles. This underscores the need for further research in this largely unexplored area.

- Morphological characteristics: in order to be used as efficient drug carriers, MOFs for preparing CHs-MOFs are also selected based on their pore types and volume. Generally, the larger the pore volume, the greater the capacity for drug

loading, including the accommodation of large molecules. Additionally, the choice of MOFs depends on their versatility in modifying both external and internal surfaces. For example, pores can be made hydrophobic to load hydrophobic drugs (if they are not already), or the external surface can be functionalized with ligands for targeted delivery.

### Synthetic strategies for CHs-MOFs

As illustrated in Fig. 1, CHs-MOFs are prepared using two main approaches: post-synthetic modification (PSM), which includes physical adsorption and chemical conjugation, forming CHs-on-MOFs, and incorporation during MOF synthesis, either through encapsulation, forming CHs@MOFs, or using CHs as building units coordinated with metal nodes or ions. Regardless of the chosen synthetic strategy, CHs-MOFs are synthesized using widely adopted techniques for producing MOFs in biomedical applications. These methods are summarized in Table 1, outlining the key advantages and disadvantages of each.

In terms of PSM techniques, a straightforward approach involves immobilizing CHs onto MOF surfaces through physical adsorption. However, this method is constrained by the structures and pore sizes of the MOFs, as well as by the weak

Table 1 Main synthetic techniques for the preparation of MOFs

Synthetic methodology	Features	Advantages	Limitations	Example of MOFs
Solvothermal	<ul style="list-style-type: none"> <li>– High temperature and/or pressure</li> <li>– Solvent-driven crystallization</li> </ul>	<ul style="list-style-type: none"> <li>– High-quality, crystalline MOFs</li> <li>– Tuneable size and porosity</li> </ul>	<ul style="list-style-type: none"> <li>– Long reaction times</li> <li>– Energy-intensive</li> <li>– Use of solvents</li> <li>– Limited to water-soluble precursors</li> <li>– Less control over pore size and crystallinity</li> </ul>	<ul style="list-style-type: none"> <li>– UiO-66</li> <li>– HKUST-1</li> <li>– PCN-222</li> <li>– MIL-101(Fe)</li> <li>– ZIF-8</li> </ul>
Hydrothermal	<ul style="list-style-type: none"> <li>– Water as the solvent</li> <li>– High pressure</li> </ul>	<ul style="list-style-type: none"> <li>– Environmentally friendly</li> <li>– Lower toxicity</li> </ul>		
Microwave-assisted	<ul style="list-style-type: none"> <li>– Rapid heating</li> <li>– Uniform energy distribution</li> <li>– Short reaction time</li> </ul>	<ul style="list-style-type: none"> <li>– Cost-effective</li> <li>– Fast reaction</li> <li>– Energy-efficient</li> <li>– Uniform crystal growth</li> </ul>	<ul style="list-style-type: none"> <li>– Limited scalability</li> <li>– Expensive setup</li> <li>– Control to avoid uneven heating</li> </ul>	<ul style="list-style-type: none"> <li>– CD-MOFs</li> </ul>
Electrochemical	<ul style="list-style-type: none"> <li>– Involves electrochemical reduction of metal ions</li> <li>– Room temperature</li> </ul>	<ul style="list-style-type: none"> <li>– No solvents or additives needed</li> <li>– High crystallinity</li> <li>– Fast and energy-efficient</li> <li>– Solvent-free</li> </ul>	<ul style="list-style-type: none"> <li>– Limited range of MOFs</li> <li>– Requires specialized equipment</li> <li>– Poor scalability</li> <li>– Limited range of MOFs</li> </ul>	<ul style="list-style-type: none"> <li>– MIL-101(Fe)</li> </ul>
Mechanochemical	<ul style="list-style-type: none"> <li>– Uses mechanical force to induce reactions</li> <li>– Solvent-free or minimal solvent use</li> </ul>	<ul style="list-style-type: none"> <li>– Fast and cost-effective</li> <li>– Simple equipment</li> <li>– Short synthesis time</li> <li>– High crystallinity</li> <li>– Can improve yields</li> </ul>	<ul style="list-style-type: none"> <li>– Lower crystallinity and porosity</li> </ul>	<ul style="list-style-type: none"> <li>– HKUST-1</li> </ul>
Sonochemical	<ul style="list-style-type: none"> <li>– Ultrasonic waves create localized high-energy conditions to drive the reaction</li> </ul>		<ul style="list-style-type: none"> <li>– Requires specialized equipment</li> <li>– Difficult to scale up</li> </ul>	<ul style="list-style-type: none"> <li>– ZIF-67</li> </ul>
Spray-drying	<ul style="list-style-type: none"> <li>– Aerosolized droplets to form MOF particles in a continuous flow system</li> </ul>	<ul style="list-style-type: none"> <li>– Rapid synthesis</li> <li>– Scalable for industrial applications</li> <li>– Potential for producing uniform particles</li> </ul>	<ul style="list-style-type: none"> <li>– Limited control over crystallinity</li> <li>– Not ideal for producing highly crystalline MOFs</li> </ul>	<ul style="list-style-type: none"> <li>– UiO-66</li> <li>– ZIF-8</li> </ul>
Microemulsion technique	<ul style="list-style-type: none"> <li>– Microemulsions are the reaction media containing metal ions and organic linkers</li> </ul>	<ul style="list-style-type: none"> <li>– Control over particle size and morphology</li> <li>– Facilitates the synthesis of nanostructured MOFs</li> <li>– Can be performed under mild conditions</li> </ul>	<ul style="list-style-type: none"> <li>– Requires careful optimization of surfactants and conditions</li> <li>– Challenges in scalability</li> </ul>	<ul style="list-style-type: none"> <li>– ZIFs</li> </ul>
Vapor diffusion method	<ul style="list-style-type: none"> <li>– Diffusion of vapor phases to promote crystal growth</li> </ul>	<ul style="list-style-type: none"> <li>– Mild conditions</li> <li>– Potential high-quality crystals</li> </ul>	<ul style="list-style-type: none"> <li>– Slow crystallization</li> <li>– Difficult to control the nucleation</li> </ul>	<ul style="list-style-type: none"> <li>– UiO-66</li> <li>– CD-MOFs</li> </ul>



interactions between the MOFs and CHs (VdW and electrostatic), which are easily broken. Alternatively, CHs can be linked to MOFs *via* chemical conjugation techniques, allowing for the formation of stronger bonds (such as hydrogen, ionic, or covalent bonds). This can be achieved by functionalizing MOFs with specific groups, utilizing building units already containing these groups, such as aminoterephthalic acid instead of terephthalic acid, or by modifying the MOF surface with additional compounds. The latter method may involve anchoring organic ligands, such as PEGs, with one end having an affinity for the MOF (*e.g.*, phosphate or sulfate) and the other end capable of linking to carbohydrates, such as azides for click chemistry.

Regarding the incorporation of CHs during MOF synthesis, the first approach involves synthesising the MOF in a solution containing CHs, leading to their encapsulation or embedding within the MOF structure. Alternatively, CHs can serve as fundamental building blocks for constructing bio-MOFs, acting as organic ligands coordinated with metal nodes, as in the case of cyclodextrin-based MOFs (CD-MOFs).

To rigorously prove and thoroughly investigate the effective formation of CHs-MOFs, a comprehensive sequence of characterization techniques is essential. However, despite the critical importance of these techniques, many studies in the literature employ only a subset, thereby limiting the full characterization of CHs-MOFs and hindering their potential exploitation. Among all, infrared/Raman spectroscopy is used to identify functional groups and assess interactions between CHs and the MOFs. X-ray photoelectron spectroscopy (XPS) offers information about the elemental composition and chemical states of the loaded materials, allowing the loading of CHs to be quantified, and an understanding of their bonding with the MOFs. Energy dispersive X-ray spectroscopy (EDX) coupled with scanning electron microscopy (SEM) provides imaging and elemental analysis at the microstructural level, revealing the distribution of CHs within the MOF matrix. Inductively coupled plasma mass spectrometry (ICP-MS) is instead employed to determine the concentration of metal ions and assess the overall composition, ensuring the integrity of the MOF structure after loading. Nuclear magnetic resonance (NMR) spectroscopy can provide detailed information about the local environment of the CHs, helping to confirm their incorporation into the MOF structure and elucidate their interactions at the molecular level.

**PSM.** In a first approach for preparing CHs-on-MOFs by PSM, different CHs can be deposited onto the MOF surfaces, or, in other words, the MOF can be coated with CH.<sup>35</sup> This requires a post-synthetic treatment, in which the CHs are employed as functionalising agents of the previously-synthesized MOF.<sup>62</sup> This can be done directly using a specific CH, a modified CH with selected functional groups, or by using ligands or molecules containing CHs. The interaction between this functionalising agent and the MOF surface can thus be of low/medium energy, including hydrophilic and hydrophobic interactions, hydrogen bonds, electrostatic and VdW, but also of covalent nature.<sup>63</sup> When the formation of covalent bonds is not required, the functionalizing of the MOFs is mainly based on the diffusion of the CH (or modified CH, or ligand

with CH) to the surface of the MOFs in a solution, sometimes under mixing.

Polysaccharides/glycans such as chitosan, hyaluronic acid and heparin can directly be used, thanks to the chemical groups or charge showing affinity for the MOF surface. In general terms, the functionalization of MOFs with high molecular weight polysaccharide provides them with additional stability and may prevent MOF degradation.<sup>35</sup> Among all, hyaluronic acid (HA) is one of the most studied polysaccharides for the preparation of CHs-on-MOFs, and can be incorporated onto the MOF surface by a simple chelation reaction thanks to the large amount of carboxyl groups, resulting in NPs with improved tumour targeting ability, blood circulation time and biodistribution. HA is particularly noteworthy for its targeting abilities, especially in the context of cancer cells, including triple-negative breast cancer (TNBC).<sup>64</sup> For example, the functionalization with HA has been reported for the Zr-based porphyrinic MOF PCN-224 (Fig. 4(A)),<sup>51</sup> PCN-222,<sup>65</sup> MIL100(Fe),<sup>66</sup> and ZIF-8.<sup>67</sup> In these cases, the loading of the MOF NPs with HA acid gives rise to a drug carrier to target cancer cells overexpressing CD44 receptor.<sup>68</sup> The coating with HA has been also performed with a Zr clusters-thiazolothiazole based MOF,<sup>68</sup> and a  $\text{Fe}^{2+}$ -based MOF, the latter associated with an electrostatic adsorption.<sup>69</sup> HA can also be incorporated onto polydopamine-coated MOFs, *via* a  $\text{Fe}^{3+}$ -mediated coordination reaction, as reported for a Zn-based ZIF-8 MOF.<sup>70</sup>

Carboxymethyl cellulose and its derivatives can also be used to enhance the stability and biocompatibility of MOFs. This is the case for MIL-100(Fe) covered by carboxymethyl-dextran capable of specific targeting and killing of HER2/neu-positive cancer cells *in vitro*.<sup>73</sup> With a similar approach, a Cu-based MOF was also covered with carboxymethylcellulose, to provide better protection against the stomach acid environments and a high stability of drug dosing of ibuprofen, used as an oral model drug.<sup>74</sup>

CHs containing sulfate groups can be used in certain cases for the coating of MOFs, provided that these groups interact with the metal centres of the MOF. An example is the case of heparin, a GAG containing numerous sulfate groups, that was absorbed on iron at defect sites in the MIL-101(Fe) in a post-synthesis step (Fig. 4(B)), giving rise to a composite biomaterial with good anticoagulant activity.<sup>71</sup> Analogously, folic acid conjugated chitosan, a semi-synthetically derived amino polysaccharide with cationic character, has also been used for the functionalization of the Zr-based MOF-808, after the incubation of the modified polysaccharide with the MOF.<sup>75</sup> In other cases, the CH is incorporated into an organic ligand, often of polymeric nature, which can be later attached to the MOF structure. For example, a poly(acrylic acid-mannose acrylamide) (PAA-MAM) glycopolymer containing mannose was incorporated into MOF-808, a Zr-linked MOF. This glycopolymer was synthesised *via* RAFT polymerization of  $\alpha$ -mannose acrylamide and acrylic acid, and contains a high number of carboxylate moieties to coordinate to the  $\text{Zr}_6$  units at the particle surface (Fig. 4(C)). The final NPs were obtained after incubation of the MOF and the glycopolymer in methanol. This was reported to be associated with an increase in the NP cellular uptake.<sup>27</sup>



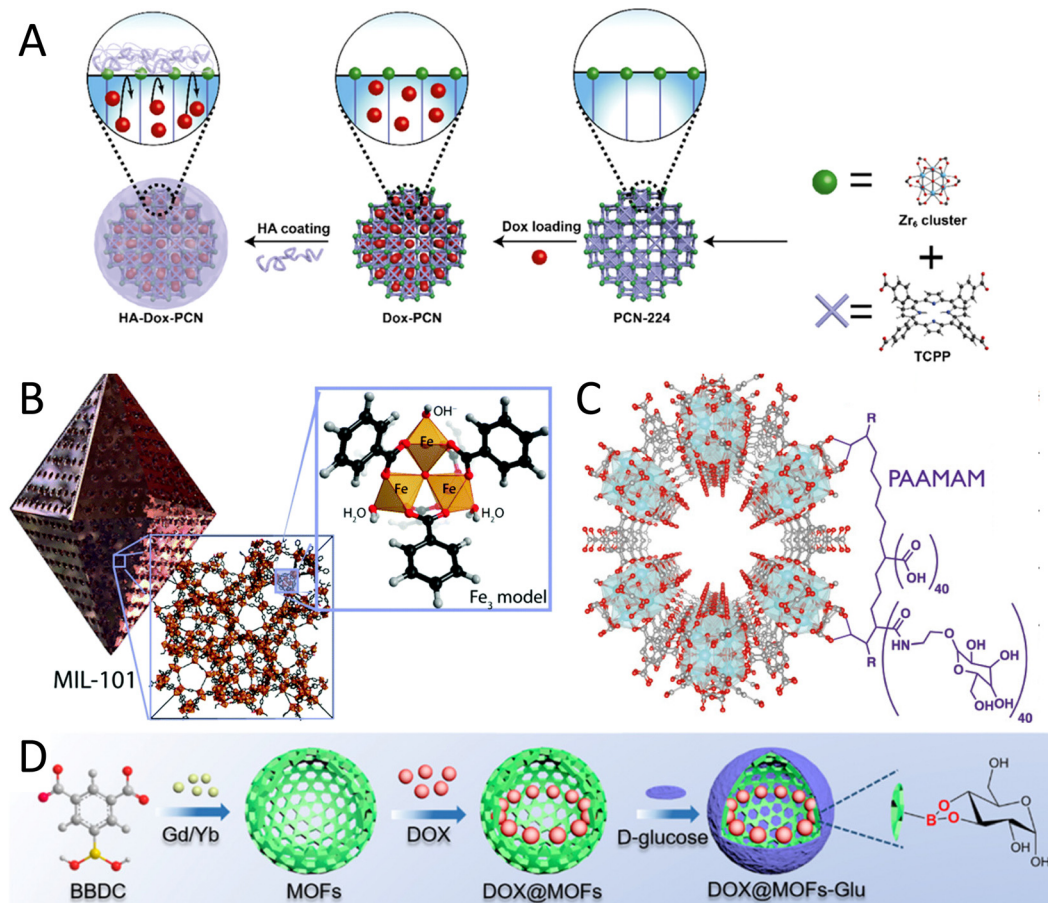


**Fig. 4** Examples of CH-on-MOF nanostructures. (A) Coating of the PCN-224 nanoMOF with HA, via their carboxylate groups. Taken from ref. 51 and reproduced with permission from the American Chemical Society, copyright 2019. (B) Heparin is able to complex with the metal sites of the MIL-101(Fe) MOF thought its sulfate groups. Taken from ref. 71 and reproduced with permission from the Royal Society of Chemistry, copyright 2018. (C) A poly(acrylic acid-mannose acrylamide) (PAAMAM) glycopolymer containing carboxylate groups is used for the functionalization of the MOF-808. Taken from ref. 27 published by the American Chemical Society, copyright 2022. (D) Synthesis of a MOF-glucose nanocarrier loaded with DOX. Taken from ref. 72 and reproduced with permission from the American Chemical Society, copyright 2018.

Some monosaccharides can also be attached to the surface of MOFs through chemical or electrostatic interactions. The incorporation of these compounds is particularly advantageous for targeting various overexpressed receptors, thereby enhancing the cellular uptake of nanoparticles by facilitating endocytosis and the effective internalization of therapeutic agents. Importantly, most CHs-MOFs made with monosaccharides, especially those designed for targeting applications, primarily utilize commercially available CHs directly linked to the MOFs, or employ short chemicals as linking agents, without further modifications. While this approach has driven valuable research and contributed to the advancement of innovative nanosystems, it also poses a limitation on ground-breaking discoveries. It does not fully leverage the rich chemistry of CHs for more efficient and selective targeting. Indeed, using simple monosaccharides does not guarantee optimal bio-interactions with targets, which often require substantial chemical modifications, such as the introduction of more polar or nonpolar functional groups. Furthermore, the absence of specific spacers between the monosaccharides and the MOFs creates significant

steric hindrance, further reducing selectivity to targeting sites. This is the case, for example, of a MOF consisting of  $\text{Gd}^{3+}$  nodes and 5-boronobenzene-1,3-dicarboxylic acid (BBDC) functionalised with glucose (Fig. 4(D)).<sup>72</sup> This nanoplatform was used for imaging-guided precise chemotherapy by interaction with glucose-transported protein (GLUT1) overexpressed in cancer cells.

Similarly,  $\text{Fe}_3\text{O}_4$  NPs were first coated with the  $\text{NH}_2\text{-MIL-100}$  MOF, and this hybrid system was subsequently incubated with  $\text{D}$ -mannose in phosphate buffered saline. The monosaccharide was eventually absorbed onto the nanostructure surface, very likely driven by an electrostatic interaction, and this nanosystem was used for the targeted therapy of tumour cells exhibiting high levels of mannose receptor (MR) expression.<sup>76</sup> In another work, a novel CaCu-MOF was firstly loaded with doxorubicin and ovalbumin, thus covered and functionalized by galactosamine-linked HA (Fig. 5(C)). The presence of HA guaranteed the biocompatibility and stability of the MOF, while the galactosamine was aimed at the targeting of the asialoglycoprotein receptor (ASGPR) overexpressed on hepatic cancer cells.<sup>77</sup> In all



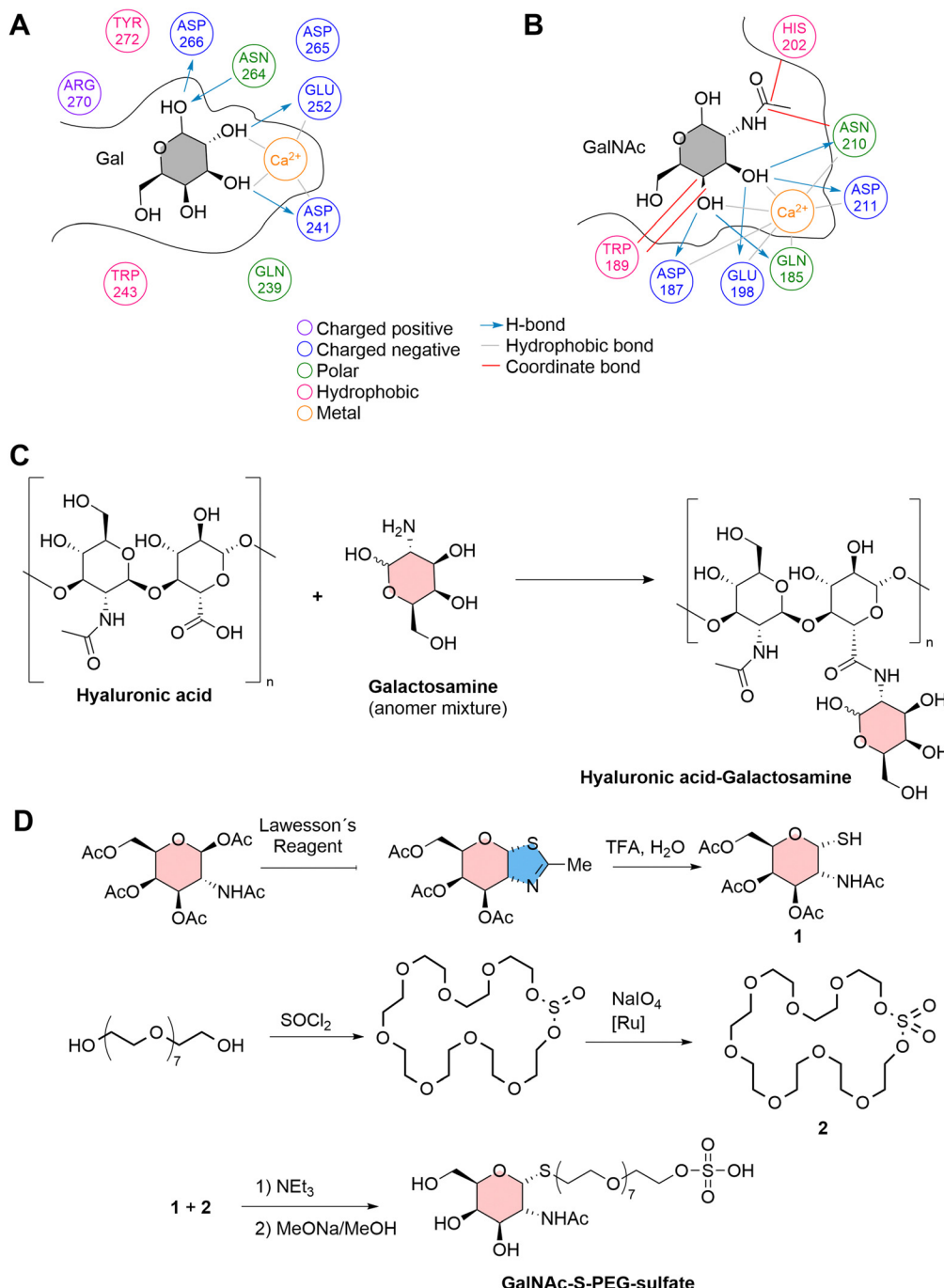


**Fig. 5** Molecular interactions between (A) galactose, and (B) *N*-acetyl-galactosamine (GalNAc) at the active binding site (CRD) of ASGPR. (C) The preparation of HA-galactosamine for the functionalization of CaCuMOF.<sup>77</sup> (D) Synthetic strategy for the preparation of a ligand based on *N*-acetylgalactosamine and sulphated PEG for the functionalization of PCN-222.<sup>11</sup>

these examples, no chemical modification of the monosaccharides was performed (except for those required to link them to the MOFs), nor were any specific spacers used between the monosaccharide and the MOF. This limitation affects targeting capabilities. For instance, in the case of targeting the ASGPR, it has been demonstrated that the structural characteristics of the

monosaccharides are critical for interaction with the C-terminal carbohydrate recognition domain (CRD) of ASGPR. Specifically, the CRD of ASGPR comprises the amino acids aspartic acid 241, aspartic acid 265, asparagine 264, glutamic acid 252, glutamine 239, and tryptophan 243.<sup>78</sup> CHs binding is initiated by the coordination of specific amino acids in the



receptor with  $\text{Ca}^{2+}$  ions, facilitating the binding of hydroxyl moieties (Fig. 5(A)). The binding of ASGPR ligands is influenced by several factors including the proximity of  $\text{Ca}^{2+}$  to two oxygen atoms (preferably the 3-OH and 4-OH groups) of the sugar, which allows for coordinate bond formation, the orientation of the pyranose ring of the sugar to maximize hydrophobic interactions between tryptophan 243, and the carbon atoms of the ligands (C3–C6), and numerous hydrogen bonds that stabilize ligands at the binding site.<sup>78</sup> As shown in Fig. 5(B), this binding is particularly enhanced when using specifically designed CHs, such as *N*-acetyl-galactosamine.

For example, in a recent study, a polyethylene glycol (PEG) ligand was synthesized with thio-*N*-acetylgalactosamine linked through C1 at one end and a sulfate group at the other end. This ligand was then attached to PCN-222 through interactions between the sulfate group and Zr nodes, utilizing a continuous flow reactor. The presence of a spacer with specific length allowed avoiding steric hindrance limitations, leaving the external *N*-acetylgalactosamine free to potentially interact with ASGPR with enhanced interactions compared with pure galactosamine (Fig. 5(D)).<sup>11</sup>

In another peculiar investigation, the possibility of using amphiphiles for the functionalization of hydrophobic MOFs, rendering water-dispersible nanosystems, was also explored. This strategy has been employed for the stabilization of ZIF-8, a hydrophobic MOF,<sup>79</sup> which after incubation with an alkyl-polyglucoside such as *n*-dodecyl  $\beta$ -D-maltoside, gives rise to water-dispersible micelles (Fig. 6(B)).<sup>80</sup> This glyco-MOF nanosystem contains maltose-exposing sugar moieties, and this strategy can thus be used to obtain colloidal suspensions of nonpolar nanoparticles in polar solvents.<sup>33,57,75,77</sup>

Aiming at establishing more robust CH-MOF interactions, researchers also explored bioconjugation reactions, sometimes referred as to grafting. CHs-MOFs prepared by bioconjugation show the advantage of enhanced thermal and mechanical resistance. For example, hyaluronic acid (HA), a nonsulfated GAG, has been conjugated with a ZIF-8 derived nanostructure which contains hydrophilic carboxylic acid groups in the MOF

organic linkers. Standard EDC/NHS chemistry (*i.e.*, the formation of amide bonds from carboxyl and amine groups) was employed, resulting in the synthesis of HA/ZIF-8 films with antibacterial properties.<sup>82</sup> With another approach, MIL-101(Fe) surfaces were functionalized with the GAG heparin, normally used as an anticoagulant agent, to enhance colloidal stability across various biological environments.<sup>83</sup> The heparin-functionalized MIL-100(Fe) (HP-on-MIL-100(Fe)) exhibited a drug loading capacity reaching up to 42 wt% using caffeine as a model drug. Additionally, HP-on-MIL-100(Fe) provided superior control over the drug release compared to the uncoated MIL-100(Fe). A similar strategy has been reported for the incorporation of galactose and mannose to the  $\text{NH}_2$ -MIL-53(Fe) surface. This MOF contains 2-aminoterephthalic acid ( $\text{NH}_2$ -BDC) linkers, which are used for the conjugation with 4-aminophenyl- $\beta$ -D-galactopyranoside and 4-aminophenyl- $\alpha$ -D-mannopyranoside after the MOF synthesis, in the presence of glutaraldehyde. The authors eventually obtained a glyco-MOF with applications in the sensing and detection of bacteria.<sup>84</sup> Analogously,  $\text{NH}_2$ -MIL-101(Fe) nanoparticles treated with hyaluronic acid in the presence of EDC result in a hybrid HA-on-MIL nanosystem in which the -COOH groups of polysaccharides and the -NH<sub>2</sub> groups of the MOF form an amide bond. In particular, this carrier can be loaded with platinum-based drugs for targeted cancer therapy (Fig. 6(A)).<sup>81</sup> The  $\text{NH}_2$ -MIL-101 MOF can also be suitable for click chemistry conjugation. For example, a first conversion of the amino to an azide group followed by a reaction with 1-propargyl-O-maltose gave rise to a maltose-on-MOF with applications in the fast determination of small biomolecules.<sup>85</sup>

Similarly,  $\text{NH}_2$ -UiO66 was functionalized with D-mannose by reductive amination using sodium triacetoxyborohydride as the reducing agent,<sup>86</sup> and sequentially the recombinant human bleomycin hydrolase (rhBLMH) was encapsulated. When the resulting nanosystems were administered intratracheally, the nanoparticles entered epithelial cells, protecting the lungs from pulmonary fibrosis during bleomycin-based chemotherapies. Encapsulating rhBLMH in MHP-UiO-66 also shielded the enzyme from proteolysis and improved cellular uptake.

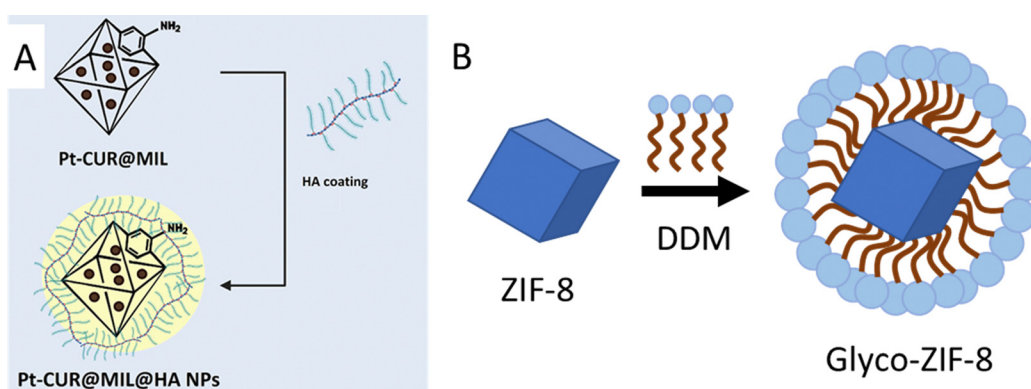


Fig. 6 (A) Conjugation of platinum-curcumin ( $\text{NH}_2$ -MIL-101(Fe)) nanoparticles and hyaluronic acid. Amino groups belonging to the ligand 2-aminoterephthalic acid react with -COOH groups of hyaluronic acid, in the presence of EDC/NHS. Taken from ref. 81 and reproduced with permission from John Wiley & Sons Ltd, copyright 2022. (B) Functionalization of ZIF-8 NPs with the amphiphile *n*-dodecyl  $\beta$ -D-maltoside (DDM), resulting in water-dispersible glyco-ZIF-8 micelles exposing carbohydrate moieties. Adapted from ref. 80 published by the American Chemical Society, copyright 2019.



Table 2 Selected publications related to CHs-MOFs prepared by PSM

CHs	MOF	Role of CHs	Aim of CHs-MOFs	Ref.
Heparin	MIL-101(Fe)	Anticoagulant for PTFE implant	Controlled release of heparin during degradation	71
Heparin	MIL-100(Fe)	Evasion from the recognition by immune cells	Controlled release of caffeine (model drug) and furazan-derivate (antitumoral)	83
Heparin	Fe-MOF	Increase the accumulation and luminescent intensity	Piezoelectric-Fenton-photodynamic images (theragnostic)	88
Hyaluronic acid	ZIF-8	Antibacterial properties	Wound healing applications	82
Hyaluronic acid	MIL-100(Fe)	Targeting of cancer cells	Delivery of indocyanine green for photothermal therapy	66
Hyaluronic acid	PCN-224	Increase biocompatibility, act as polymer gatekeeper and targeting cancer cells	Controlled release of doxorubicin and photodynamic therapy	51
Hyaluronic acid	PCN-224	Targeting of cancer cells	Controlled release of immunologic adjuvant (CpG) and photodynamic therapy	65
Hyaluronic acid	ZIF-8	Increase the biocompatibility, stability and targeting of cancer cells	Controlled release of chlorin e6 for photodynamic therapy	67
Hyaluronic acid	ZIF-8	Targeting of cancer cells	Controlled release of doxorubicin	70
Hyaluronic acid	MIL-101(Fe)	Increase cellular uptake	Controlled release of 5-fluorouracil (anticancer)	89
Hyaluronic acid	ZIF-8	Negative charge of the MOFs for use on contact lenses and biocompatibility	Controlled release of levofloxacin (antibacterial)	90
Hyaluronic acid	Cu/PCN-224	Improve water dispersibility and biocompatibility	Controlled release of disulfiram prodrug (anticancer)	91
Hyaluronic acid	ZIF-8	Improve the stability	Controlled release of evodiamine (anticancer)	92
Hyaluronic acid	UiO-66	Increase stability and cellular uptake	Controlled release of 5-fluorouracil (anticancer)	93
Hyaluronic acid	Fe/Cu-MOF	Increase stability and cellular uptake	Controlled release of lactate oxidase and Fe/Cu for chemodynamic therapy	94
Hyaluronic acid	Zr-MOF	Targeting of cancer cells	Photo dynamic therapy	68
Hyaluronic acid	Fe-MOF	Targeting of cancer cells	Photo dynamic therapy	69
Hyaluronic acid	MIL-101(Fe)	Increase stability and biocompatibility	Controlled release of platinum-curdum	81
Hyaluronic acid	ZrTc MOF	Targeting of cancer cells	Hydrogen therapy	95
Hyaluronic acid	ZIF-8	Targeting of cancer cells	Controlled release of cisplatin (CDDP) and SR-717 (a STING agonist)	96
Hyaluronic acid	Ag <sub>2</sub> S/ZIF-8	Targeting of cancer cells	Controlled release of doxorubicin and photodynamic therapy	97
Hyaluronic acid	Fe-MOF	Targeting of cancer cells	Controlled release of L-buthionine sulfoximine (BSO) and chlorin e6 for photodynamic therapy	98
Hyaluronic acid	Fe-MOF	Targeting of cancer cells	Controlled release of Fe (Fenton reaction), oxaliplatin and L-arginine	99
Hyaluronic acid (sulfonated)	Cu-MOF	Anticoagulant and anti-inflammatory	Improve the biocompatibility of implant materials.	100
Galactosamine-linked	CaCu-MOF	Increase stability	Controlled release of doxorubicin and Cu for chemodynamic therapy	77
hyaluronic acid	MIL-100(Fe)	Increase stability and biocompatibility	Controlled release of daunorubicin (anticancer)	73
Carboxymethyl-dextran				
Phosphated cyclodextrins	MIL-100(Fe)	Increase stability	Potential drug delivery system	29
Carboxymethylcellulose	Cu-MOF	Increase stability in PBS	Controlled release of ibuprofen	74
Carboxymethylcellulose	UiO-66-NH <sub>2</sub>	Increase stability in PBS	Controlled release of 3,4-dihydroxybenzaldehyde (DHBD) drug and 5-fluorouracil	101
Chitosan- <i>graft</i> -poly (lactic acid)	CD/MOF	Increase solubility	Controlled release of curcumin (as a model water insoluble drug)	102
Chitosan	MIL-100 (Fe)	Increase resistance to degradation	Controlled release of piperine (anticancer)	103
Chitosan	Cu-MOF	Increase biocompatibility	Controlled release of doxorubicin (anticancer)	104
Chitosan	Ca-MOF	Increase biocompatibility	Controlled release of Ca and alendronate for bone engineering	105
Chitosan	MOF-808	Improve stability	Controlled release of quercetin (QU)	75
Cellulose/chitosan	MOF-199	Support media for MOF	Extraction of benzodiazepines (BZPs) from urine	106
B-cyclodextrin	MOF-235	Increase luminescent intensity	Glucose detection in human serum	107
D-Mannose	Fe-MOF	Targeting of cancer cells	Controlled release of doxorubicin and methotrexate	108
D-Mannose	MIL-100(Fe)	Targeting of cancer cells	Applications for chemodynamic therapy (CDT)	76
D-Mannose	UiO-66	Targeting of cancer cells	Controlled release of recombinant human bleomycin hydrolase (rhBLMH) to prevent pulmonary fibrosis	86
Mannosamine	MIL-88A(Fe)	Targeting of cancer cells	Internalization in alveolar macrophages	109
D-Mannose (poly(acrylic acid-mannose acrylamide))	MOF-808	Targeting of cancer cells	Controlled release of both carboplatin and flouxuridine	27
Glucose	Gd-MOFs	Increase biocompatibility, act as gatekeeper and targeting cancer cells	Controlled release of doxorubicin	72



Table 2 (continued)

CHs	MOF	Role of CHs	Aim of CHs-MOFs	Ref.
Galactose and mannose	MIL-53(Fe)	Targeting receptors of bacteria	Detection of <i>P. aeruginosa</i> and <i>E. coli</i>	84
Galactose	PCN-224	Targeting of cancer cells	Controlled release of doxorubicin and photo dynamic therapy	87
Galactose	ZnAP-MOF	Targeting of cancer cells	Controlled release of 6-allylthiopurine (6-AP)	110
<i>N</i> -Acetylgalactosamine	PCN-222	Targeting of cancer cells	Potential drug carrier and photodynamic therapy	11
Maltose ( <i>n</i> -dodecyl $\beta$ -D-maltoside)	ZIF-8	Stability and potential targeting	Potential drug carrier	80
Maltose	MIL-101	Ultrahigh ionization efficiency, free matrix background, uniform crystallization, and good dispersibility	Determination of small biomolecules by laser desorption ionization mass spectrometry (LDI-MS)	85

The nanoparticles also boosted pulmonary accumulation of rhBLMH, offering more effective lung protection during chemotherapy.

A combination of bioconjugation and the formation of weaker interactions has been employed for the incorporation of galactose to the PCN-224 surface. In the first step, after the MOF synthesis, the NPs were coated with polyethylene glycol with carboxylate terminals (COOH-PEG-COOH) through electrostatic adsorption. These NPs thus exhibited -COOH on their surface, which reacted with amine-modified galactose in the second step, using ethyl-(dimethylaminopropyl)carbodiimide (EDC) as a coupling agent. This hybrid nanosystem was used for the targeted photodynamic and chemotherapy therapy of hepatocellular carcinoma.<sup>87</sup> A relatively high number of other studies have reported novel CHs-MOFs systems prepared by PSM. Some of the most recent and relevant are reported in Table 2.

**Incorporation of CHs during the synthesis of MOFs.** The encapsulation of carbohydrates by MOFs, the so-called CH@MOF structures, are usually employed to preserve the biological activity of biomolecules,<sup>111</sup> avoiding also their leaching before reaching the site of action (in the context of nanoparticles, “@” is commonly used to denote a core–shell structure or encapsulation, where one material – normally the first one in order – is coated or surrounded by another – the one after the @). Analogously to other biomolecules, CH and CH-based drugs can be encapsulated into the cavity of the MOFs, producing in many cases structurally stable host–guest ensembles. To date, this strategy has been limited to few polysaccharides, such as HA, chondroitin sulfates, dermatan sulfates, keratin sulfates and heparan sulfates. Recently, glycosaminoglycans (GAG) containing heparin (HP), HA, chondroitin sulfate (CS), and dermatan sulfate (DS) were also encapsulated in Zn-azolate frameworks ZIF-8, ZIF-90, and MAF-7 through a one-pot strategy, resulting in GAG@MOF biocomposites. The hybrid CH@MOF nanostructures were synthesised in aqueous solutions from their Zn precursors and the corresponding ligands in the presence of the carbohydrates (Fig. 7(A)).<sup>112</sup>

Carboxylate-functionalized dextran has also been encapsulated into ZIF-8 pores. The modified polysaccharide was used as biomimetic mineralisation agents for the formation of CHs@ZIF-8 biocomposites, and was also added to the reaction media during the MOF synthesis. It should be noticed that the presence of carboxylate functional groups was identified as a key factor for successful encapsulation<sup>113</sup> of the polysaccharide, and that the encapsulation of monosaccharides or

oligosaccharides such as D-glucose, D-galactose, D-mannose D-xylose and sucrose was not possible (Fig. 7(B)).<sup>114</sup> Table 3 summarises other recent examples of CHs@MOFs, while a list of more dated works can be found elsewhere.<sup>35</sup>

Another approach for the preparation of CHs-MOFs by incorporating the CHs during the synthesis of MOFs, exploits the presence of reactive chemical groups of CHs capable of coordinating with inorganic metals. This approach has already resulted in different types of MOFs using lipids, proteins, and nucleic acids, but has attracted less attention and technical challenges with CHs. Currently, researchers have achieved crystalline MOFs practically only employing cyclodextrins (CD). Among most methods used for the preparation of CD-MOFs, researchers have investigated vapor-diffusion, solvothermal, liquid–liquid methods, and microfluid synthesis. Recently, CD-MOFs based on  $\gamma$ -CD were prepared by an ultrasonic-assisted solvothermal method, obtaining uniformly-sized nanoscale edible NPs, avoiding the issue of poor size distribution, one of the most common problems of CD-MOFs.<sup>116</sup> The NPs were further modified by ester bond cross-linking, to obtain a nanosystem capable of loading quercetin, a naturally occurring flavonoid bioactive compound, that has antioxidant, anti-inflammatory, and anticancer effects. The CD-MOF showed storage stability for 14 days, and enhanced biocompatibility. CD-MOFs were also prepared using a stream diffusion method using green chemistry principles, followed by loading with apigenin, a potential bioactive functional food ingredient.<sup>117</sup> As mentioned in the introduction, reviews related to CD-MOFs and recent trends in this field have already been reported in the literature and are not here repeated.<sup>26,45–47</sup> Another strategy that can be somehow classified as a type of methodology using CHs as building units, is the use of CHs as a sort of template for the controlled growth of MOFs. This is the case in the preparation of HKUST-1 and ZIF-8 with chitosan,<sup>114</sup> and some examples in which fructose is used as the MOF organic linker in  $\text{Sr}^{2+}$  and  $\text{Ca}^{2+}$  based MOFs have also been reported in the literature.<sup>119,120</sup> However, in general, the preparation of CHs-MOFs using CHs during the synthesis of MOFs is less explored to date and, especially in the case of using CHs as building units, practically limited to the use of CDs, as summarized in Table 3.

## Advancements in preclinical evaluations of CHs-MOFs

Over the past few years, some different CHs-MOFs have already been tested in preclinical trials. While their application in



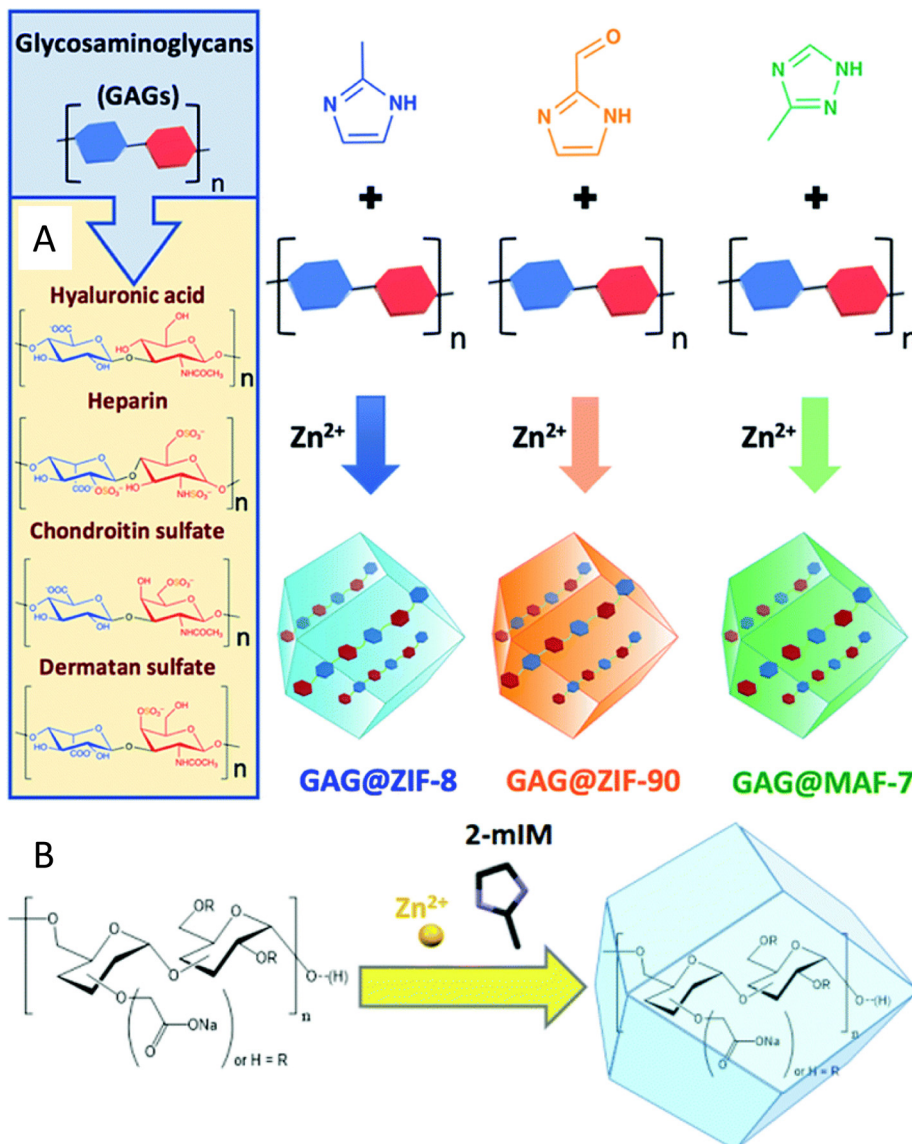


Fig. 7 Encapsulation of carbohydrates (polysaccharides) in MOF pores. (A) One-pot synthesis of glycosaminoglycans GAG@MOF biocomposites based on three different metal-azolate frameworks. Taken from ref. 112 published by the Royal Society of Chemistry. (B) Biomimetic mineralisation of carboxylated-dextran@Zn(2mIM)<sub>2</sub>. In both cases the MOFs are synthesised from their metal precursor and organic ligands in the presence of the carbohydrates. Taken from ref. 113 published by the Royal Society of Chemistry.

industrial settings still requires further validation, these trials have confirmed their potential for biomedical use. One notable example is MIL-100(Fe), engineered specifically to co-deliver oxaliplatin (OXA)—a widely used platinum-based chemotherapy drug for advanced colorectal cancer (CRC)—and L-arginine (L-Arg) to combat OXA resistance (Fig. 8(A)).<sup>99</sup> The synthesis of the MOF involved encapsulating both OXA and L-Arg within its porous structure, followed by surface modification with hyaluronic acid, facilitating binding to CD44 receptors. This resulted in the formation of the L-Arg&OXA@MOF-HA construct. Upon reaching the tumour site, the high levels of glutathione (GSH) characteristic of the tumour microenvironment reduce Fe<sup>3+</sup> to Fe<sup>2+</sup>, leading to the disintegration of the MOF structure and the controlled release of OXA and L-Arg.

This mechanism not only depletes intracellular GSH but also augments the cytotoxic efficacy of OXA. Furthermore, the released Fe<sup>2+</sup> initiates a Fenton reaction with endogenous hydrogen peroxide, generating hydroxyl radicals and liberating nitric oxide (NO). This cascade of reactions collectively sensitizes cancer cells and induces cell death through oxidative stress. *In vitro* experiments (Fig. 8(B)) demonstrated a significant enhancement in cytotoxicity against OXA-resistant HCT-116/L colorectal cancer cells, achieving more than 60% reduction in cell viability compared to treatment with OXA alone. Flow cytometric analysis confirmed an increase in apoptosis, with elevated levels of reactive oxygen species and NO detected in the treated cancer cells. *In vivo* studies utilizing tumour-bearing mice exhibited marked tumour inhibition,

Table 3 Selected publications related to CHs-MOFs prepared by using CHs during the synthesis of MOFs

CHs	MOF	Role of CHs	Aim of CHs-MOFs	Ref.
Encapsulated CHs				
Different polysaccharides	ZIF-8	Biomimetic mineralisation and therapeutics	Controlled release of polysaccharide-based therapeutics	113
Glycosaminoglycans (GAGs)	ZIF-8 ZIF-90 MAF-7	Therapeutics	Controlled release of GAGs	112
Fucoidan	EuMOF	Therapeutic	Controlled release of fucoidan	115
CHs as building units				
Chitosan	HKUST-1 ZIF-8	Control the biomimetic growth of MOFs	Demonstrate the polysaccharides are an excellent medium for the growth and the expansion of crystalline MOFs	114
$\gamma$ -CD	CD-MOF	Biocompatibility	Controlled release of quercetin (dietary supplement)	116
B-CD	CD-MOF	Biocompatibility	Controlled release of apigenin (dietary supplement)	117
Fructose	Sr-based MOF	Coordinate Sr ions	Promotes the encapsulation of earth alkaline ions on chitosan NPs	118

with the group treated with the CHs-MOFs showing the most pronounced tumour suppression. Notably, the nanoplatform exhibited high biocompatibility, with negligible toxicity recorded in healthy human liver cells (HL-7702) and macrophages.

In another study, UiO-66-NH<sub>2</sub> was modified *via* a Schiff base reaction with 4-dihydroxybenzaldehyde (DHBD) forming a pH-sensitive C=N bond.<sup>101</sup> This MOF was subsequently encapsulated within a hydrogel matrix composed of carboxymethyl cellulose (CMC) and alginate, yielding a dual pH-responsive delivery system designed to co-deliver DHBD@MOF and 5-fluorouracil (5-FU) for colorectal cancer therapy. The CMC coating effectively protects the drug from premature release in acidic environments such as the stomach and small intestine, facilitating the release of active agents in the neutral to slightly acidic pH of the colorectum. Preclinical release studies demonstrated that only 1.31% of DHBD was released from the hydrogel at pH 1.2 (simulating stomach acid) within 2.5 hours, thereby preventing premature drug degradation. Under tumour-like conditions at pH 6.5–7.4, however, a controlled and sustained release was achieved, with significant drug release observed over 8.5 and 24 hours. Specifically, 41.68% of the drug was released after 24 hours in the acidic microenvironment typical of colorectal cancer, with 89.40% and 58.32% of the inactive DHBD@MOF prodrug infiltrating the tumours after 8.5 hours and 24 hours, respectively. In pursuit of a similar pH-responsive strategy, FU@Eu-MOF was developed to enhance drug delivery for lung cancer therapy.<sup>115</sup> Fucoidan (FU), a bioactive polysaccharide, was encapsulated within a europium-based MOF through a one-pot synthesis. *In vitro* studies indicated that FU@Eu-MOF significantly improved cytotoxicity against A549 lung cancer cells compared to free fucoidan or Eu-MOF alone. This system achieved a high drug loading efficiency of 22.15% by weight and exhibited a controlled release profile (85.3% over 48 hours), particularly in acidic environments (pH 5–6), which mimic tumour tissues. The results demonstrated that FU@Eu-MOF exhibited enhanced anticancer potential, with an IC<sub>50</sub> value of approximately 32  $\mu$ g ml<sup>-1</sup>, compared to fucoidan alone, which had an IC<sub>50</sub> value of approximately 60  $\mu$ g ml<sup>-1</sup>. This improvement is attributed to the combination of elevated reactive oxygen species (ROS) levels leading to DNA damage and mitochondrial dysfunction-mediated apoptosis. Specifically, the extent of ROS-mediated DNA damage was

assessed in terms of the percentage of tail DNA. Vehicle control cells exhibited *ca.* 97% head DNA with only 3% tail DNA. In contrast, FU@Eu-MOF and fucoidan-treated cells showed approximately 31% head DNA and 10% tail DNA, respectively. Additionally, apoptotic cell rates in the FU@Eu-MOF and fucoidan-treated groups were recorded at approximately 82% and 48%, respectively, in contrast to only about 5% apoptotic cells in the vehicle control group (Fig. 9(A)).

Another CHs-MOFs was developed utilizing the purine nucleobase prodrug, 6-allylthiopurine (6-ATP), in conjunction with a ZnAP MOF to enhance synthetic lethal therapy in cancer treatment.<sup>110</sup> Prodrug-skeletal MOFs (ZnAP) were synthesized through a solvothermal method employing 6-AP, biphenyl-4,4'-dicarboxylic acid (4-BPA), and Zn<sup>2+</sup>. The PARP inhibitor (ANI) was conjugated with a hydrophilic chain terminated with galactose *via* an amide linkage to yield Gal-ANI, which exhibits aggregation-induced emission (AIE) to facilitate monitoring of drug uptake. Subsequently, Gal-ANI was modified onto the surface of ZnAP *via*  $\pi$ - $\pi$  stacking and hydrogen bond interactions, culminating in the construction of Gal-ANI-on-ZnAP. The incorporation of a glycosylated AIE PARP inhibitor enabled real-time visualization of drug uptake in cancer cells. *In vitro* studies revealed pH and esterase responsiveness of Gal-ANI-on-ZnAP, with 86% of ANI and 88% of 6-AP released at pH 5.0 in the presence of esterase after 48 hours, thereby minimizing toxicity to healthy cells. Fluorescence studies confirmed effective uptake of the NPs in HepG2 cells, attributed to their affinity for the asialoglycoprotein receptor (ASGPR). In contrast, negligible fluorescence was observed in HL7702 cells, which exhibit low ASGPR expression, indicating targeted delivery. Cytotoxicity assays revealed that Gal-ANI-on-ZnAP NPs were highly toxic to HepG2 cells, achieving only 13% survival at a concentration of *ca.* 90  $\mu$ g ml<sup>-1</sup> after 48 hours, while HL7702 cells maintained over 75% viability, highlighting the selective antitumor activity of the NPs. Colony formation assays further illustrated their significant antiproliferative effects. Furthermore, treatment with Gal-ANI-on-ZnAP resulted in a decreased mitochondrial membrane potential (MMP) and elevated reactive oxygen species (ROS) levels in HepG2 cells, signalling the induction of apoptosis. Flow cytometry analysis demonstrated a substantial apoptosis rate of 97.27% in treated cells,



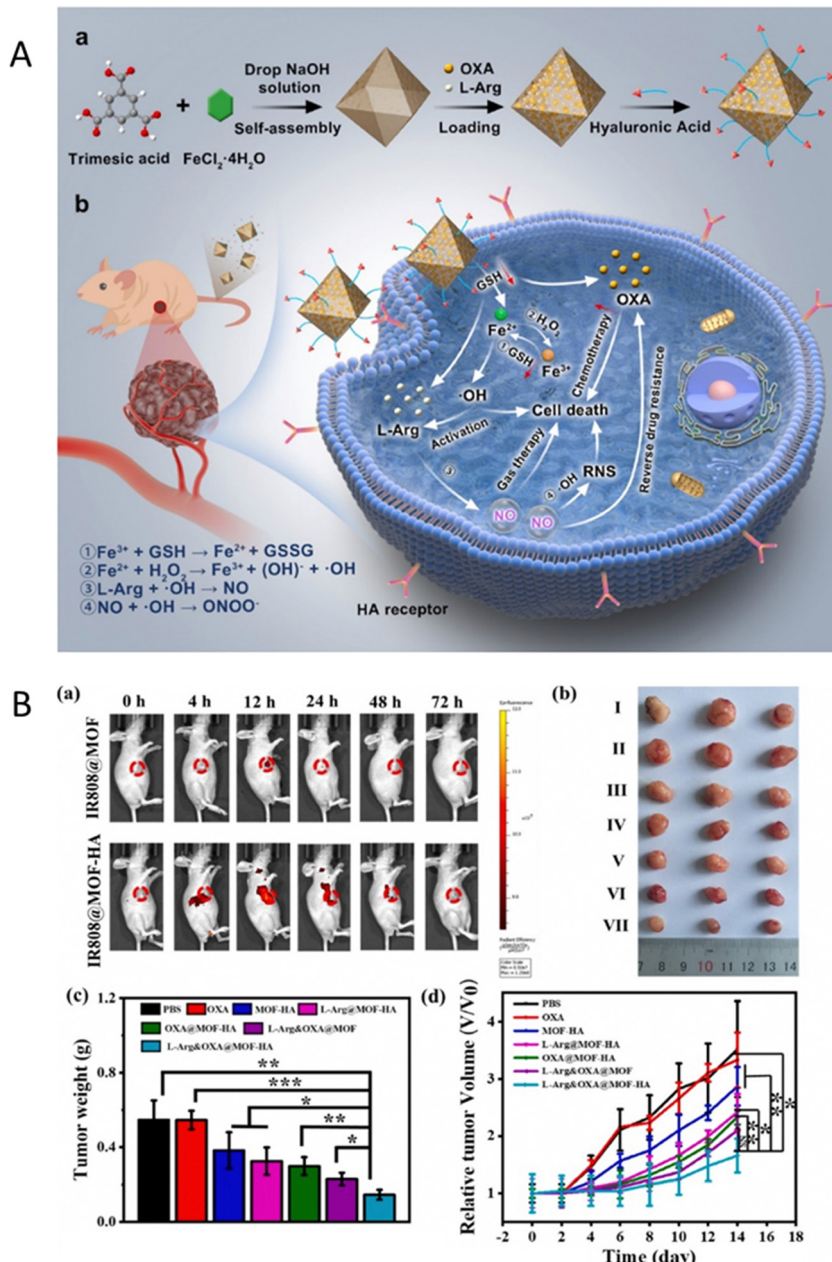


**Fig. 8** (A) (a) Preparation process of the designed nanoplatform; (b) potential mechanisms by which the nanoplatform overcomes drug resistance and exerts anti-CRC effects. (B) (a) Time-dependent *in vivo* imaging of HCT-116/L tumor-bearing mice administered MOFs via intravenous injection; (b) photographs of tumours from mice following indicated treatments (I: PBS; II: OXA; III: MOF-HA; IV: L-Arg@MOF-HA; V: OXA@MOF-HA; VI: L-Arg&OXA@MOF; VII: L-Arg&OXA@MOF-HA); (c) average tumour weights across treatment groups; (d) tumour growth profiles for mice receiving the indicated treatments. Scale bars represent 50  $\mu\text{m}$ . Reprinted and adapted from ref. 99 with permission from Elsevier, copyright 2024.

attributed to DNA damage resulting from the combined effects of ANI and 6-AP.

## Conclusions and outlook

The integration of carbohydrates into metal-organic frameworks (MOFs) creates CHs-MOFs composites exhibiting synergistic properties such as enhanced chemical and thermal stability, controlled release, and higher selectivity, which are

not observed in the individual components. Additionally, incorporating CHs into MOFs can improve the bioavailability and pharmacokinetics of carbohydrate-based therapeutics. These hybrid nanosystems have potential applications as drug delivery systems, analytical tools, and can also serve as contrast agents for imaging techniques like magnetic resonance imaging (MRI) and computed tomography (CT). The increasing number of research articles and patents highlights the growing interest and significant industrial investment in this field. For instance, CN110545793B discusses a method for preparing

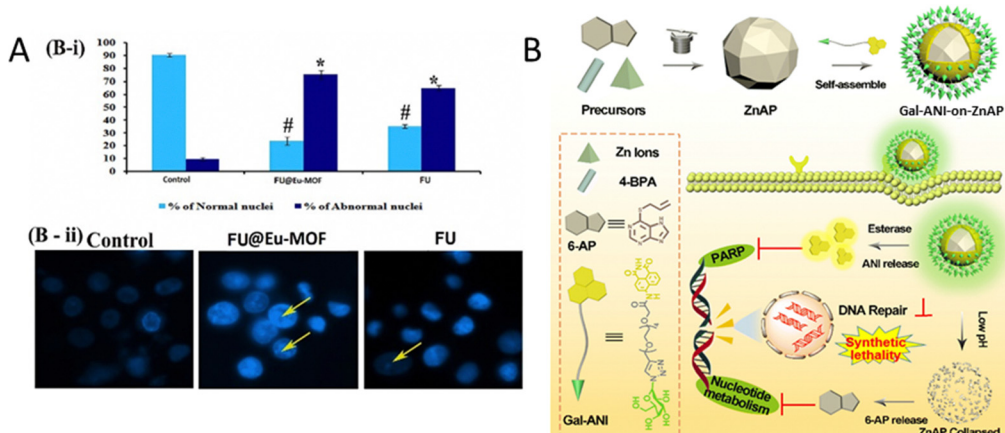


Fig. 9 (A) B: Alterations in nuclear DNA: (i) quantitative results for the number of apoptotic cells per 100 total cells, (ii) microscopic images illustrating nuclear fragmentation, DNA nicks, and nuclear deformities. Reprinted and adapted from ref. 115 with permission from Elsevier, copyright 2022. (B) Schematic illustration of the construction of Gal-ANI-on-ZnAP and its application for synthetic lethal therapy and visualization therapy adapted from ref. 110.

MOFs modified with specific ligands, including hyaluronic acid, to target CD44 receptors in tumour cells. Similarly, CN108187046B reports a MOF shielded with hyaluronic acid that can carry curcumin for both cancer diagnosis and treatment. Some other patents are related to CD-MOFs, such as US10583147B2, US9085460B2, CN107151329B, and CN107837401B. For example, US10125016B2 reports a method for the environmentally friendly synthesis of CD-MOFs, and US10500218B2 describes loading different drugs into CD-MOFs for biomedical applications.

However, despite the tremendous potential of CHs-MOFs and the burgeoning focus in the field, many challenges and limitations must be addressed to shift academic R&D results to real-world biomedical applications:

1. Scalability and reproducibility: firstly, substantial technical challenges related to the large-scale preparation of MOFs for biomedical applications need to be addressed. This includes achieving good reproducibility and yields of size-controlled MOF nanoparticle synthesis. These challenges are compounded by the poor understanding and modelling of MOF crystallization, from seed formation to growth.<sup>121</sup> Currently, most MOF-related papers are limited to synthesizing only dozens of milligrams or few grams per batch, and larger-scale productions are rarely considered,<sup>122,123</sup> and are practically unreported for biomedical applications.<sup>124</sup> This limitation should also be addressed when using intensified processes, such as continuous flow synthesis, as well as other innovative technologies like microwave and ultrasound-assisted synthesis, which are typically explored for their potential to scale-up but rarely demonstrated effectively for this purpose.<sup>125,126</sup> Reaching reliable, large-scale production methods is essential for translating CHs-MOFs from research to clinical applications.

2. Size control: achieving precise control over the size of CHs-MOFs is difficult, as size distribution is often influenced by kinetic factors, which are harder to scale up than thermodynamic control. Many studies in the literature do not address the size distribution of the produced CHs-MOFs, and only a few have investigated how various experimental conditions impact

their shape and size. For example, the first study on the effect of the different parameters on the shape and size of PCN-222 was only recently reported.<sup>11</sup> Furthermore, as mentioned earlier, the impact of the size of CHs-MOFs on ADMET should be thoroughly explored, potentially using advanced computational techniques such as machine learning (ML).

3. Sustainability characteristics: the sustainable production of MOFs should be considered, as current preparation methods are typically energy and solvent-consuming. For example, MIL-101(Fe) and PCNs are produced using DMF (*N,N*-dimethylformamide),<sup>125,126</sup> a highly toxic and potentially carcinogenic solvent. Although some articles have recently discussed environmentally friendly MOF synthesis for biomedicine, opening the research to this type of investigation, requires much more effort, including green metrics<sup>127–129</sup> and life cycle assessment (LCA) calculations.<sup>130</sup> At the same time, the well-established chemistry of carbohydrates and the production of CH-based drugs, considering the green principles of chemistry, is an advantageous point in developing CHs-MOFs. However, only a few monosaccharides have been exploited to produce CHs-MOFs, with polymeric CHs being more commonly selected. This implies limited chemical control, and the effect of different sizes of CH-polymers on bio-interactions within CHs-MOFs is not well understood.<sup>131</sup> Natural ligands should also be more extensively considered as tools for functionalizing MOFs with CHs, as demonstrated recently with a lecithin-based ligand used for the functionalization of MOFs with D-mannose.<sup>132</sup>

4. Biological interactions between CHs and MOFs: the synergy between CHs and MOFs in biological systems remains poorly understood. Investigating how these two components interact, both at the molecular level and within living organisms, is crucial for maximizing their therapeutic efficacy and ensuring their safe use. These interactions influence key factors such as targeting capabilities, biodegradability, and long-term stability in biological environments. Therefore, significant effort is required to investigate bio-CHs-MOFs interactions and design more appropriate and efficient systems, including



specifically-modified CHs for targeting, and precise linkers/spacers for the modification of MOFs, similarly to what is carried out with other types of NPs.<sup>57,133,134</sup> This will require an interdisciplinary approach, combining expertise from materials chemistry, organic chemistry, biology, and computational chemistry. While this approach is still largely unexplored, it has great potential for advancing the field.

In addition, there are specific limits related to the different methods used to prepare the CH-MOFs, that needs to be implemented. In particular:

- CHs-on-MOFs prepared through PSM by low/medium energy interactions. This simple technique avoids harsh conditions and complex synthetic procedures but results in less stable CHs-MOFs. However, CHs may be less stable than covalently linked ones, leading to leaching and decreased bioactivity over time. The process may also be less efficient due to a limited number of reactive sites, resulting in lower surface coverage and heterogeneous distribution of carbohydrates, leading to non-uniform properties.

- CHs-on-MOFs prepared through PSM by bioconjugation. CHs-MOFs produced this way are more stable, and it is easier to control the location of CHs within the MOF structure. This method offers versatility due to the wide range of available MOFs and various methods for modifying MOF surfaces. Despite these strengths, grafting presents challenges, such as ensuring covalent bond formation does not disrupt the MOF structure or compromise its properties. The synthesis process is often more complicated and time-consuming, requiring precise control over reaction conditions and purification methods.

- CHs@MOFs prepared *via* encapsulation. This method results in more durable CHs-MOFs. However, encapsulation is limited to a few CHs. The synthesis can also be challenging due to potential side reactions between CHs and the other reagents. Additionally, the stability and reproducibility can be problematic, with weak interactions potentially leading to desorption of CHs-MOFs over time.

- CHs-MOFs prepared using CHs as building blocks. This strategy is practically limited to cyclodextrin-MOFs, which are also water-soluble and thus have limited applicability for biomedical applications unless appropriately modified. The use of other types of carbohydrates to obtain crystalline MOFs remains an open challenge.

As a result, ongoing research should focus on addressing these challenges alongside new research on CHs-MOFs, potentially leading to a new era in biomedical applications. In this context, the development of CHs-MOFs is greatly enhanced through various advanced synthesis and characterization techniques that optimize the interaction between carbohydrates and MOFs, thereby improving their biomedical applications. Techniques such as layer-by-layer (LbL) assembly provides precise control over MOF coatings for applications in biosensing or drug release, and green synthesis approaches emphasize environmental sustainability by utilizing renewable materials and non-toxic solvents. Click chemistry enables efficient functionalization of MOFs with carbohydrates, enhancing their biological functionality, while electrochemical synthesis

allows for precise control of reaction conditions to optimize carbohydrate interactions. Additionally, high-throughput screening and computational design techniques accelerate the discovery and development of CHs-MOFs by enabling rapid testing and predictive modelling. Together, these methods offer a comprehensive framework for fine-tuning CHs-MOFs properties, addressing challenges related to stability, scalability, and biocompatibility for applications such as drug delivery and biosensing. The search for smart, innovative solutions to the preparation of novel CHs-MOFs could pave the way for real-world biomedical applications. Despite over 100 000 MOF structures being catalogued in the Cambridge Structural Database (CSD), and the theoretical number of possible MOF structures being nearly limitless, only two MOFs have entered human trials to date.<sup>135</sup> This limited transition to industrial production, coupled with ongoing debates about its efficiency, leaves room for ground-breaking discoveries, inviting the smartest and most creative researchers to push the boundaries of CHs-MOFs development.

## Data availability

This is a review manuscript and does not contain any primary data. All data discussed and analyzed in this review are derived from previously published studies, which are appropriately cited in the manuscript. Therefore, no new data were generated or analyzed in support of this work. The cited references provide the source of all data presented. If additional information is needed, readers are encouraged to refer to the original publications listed in the reference section.

## Conflicts of interest

There are no conflicts to declare.

## Acknowledgements

Financial support was provided by the Andalusian Ministry of Economy, Science and Innovation in the framework of the Plan Andaluz de Investigación, Desarrollo e Innovación (PAIDI 2020, programme 54<sup>a</sup> “Investigación científica e innovación,” “POSTDOC\_21\_00594”), the Spanish Ministry of Science and Innovation (Ref: PID2020-119949RB-I00), the Andalusian Ministry of Economy, Science and Innovation cofinanced by the European Regional Development Fund (ERDF) from FEDER and the European Social Fund (ESF) (PY20\_00882 and CV20-04221). The COST action CA-18132 “Functional Glyconanomaterials for the Development of Diagnostic and Targeted Therapeutic Probe” and the COST action CA-22147 “European metal-organic framework network: combining research and development to promote technological solutions” (EU4MOFs) are also acknowledged.

## References

- 1 P. Valverde, A. Ardá, N. C. Reichardt, J. Jiménez-Barbero and A. Gimeno, *MedChemComm*, 2019, **10**, 1678–1691.



2 I. Bagdonaitė and H. H. Wandall, *Glycobiology*, 2018, **28**, 443–467.

3 J. Lang, N. Yang, J. Deng, K. Liu, P. Yang, G. Zhang and C. Jiang, *PLoS One*, 2013, **8**, e73097.

4 J. E. Hudak and C. R. Bertozzi, *Chem. Biol.*, 2014, **21**, 16–37.

5 B. A. H. Smith and C. R. Bertozzi, *Nat. Rev. Drug Discovery*, 2021, **20**, 217–243.

6 S. R. Falsafi, F. Topuz and H. Rostamabadi, *Carbohydr. Polym.*, 2023, **321**, 121276.

7 A. T. Thodikayil, S. Sharma and S. Saha, *ACS Appl. Bio Mater.*, 2021, **4**, 2907–2940.

8 A. Y. Fedorov, T. N. Drebushchak and C. Tantardini, *Comput. Theor. Chem.*, 2019, **1157**, 47–53.

9 C. Tantardini, S. G. Arkhipov, K. A. Cherkashina, A. S. Kil'Met'Ev and E. V. Boldyreva, *Acta Crystallogr., Sect. E: Crystallogr. Commun.*, 2016, **72**, 1856–1859.

10 S. G. Arkhipov, P. S. Sherin, A. S. Kiryutin, V. A. Lazarenko and C. Tantardini, *CrystEngComm*, 2019, **21**, 5392–5401.

11 A. Zuliani, M. Carmen Castillejos and N. Khiar, *Green Chem.*, 2023, **25**, 10596–10610.

12 E. Romero-Ben, M. C. Castillejos, C. Rosales-Barrios, M. Expósito, P. Ruda, P. M. Castillo, S. Nardecchia, J. de Vicente and N. Khiar, *J. Mater. Chem. B*, 2023, **11**, 10189–10205.

13 J. J. Cid, M. Assali, E. Fernández-García, V. Valdivia, E. M. Sánchez-Fernández, J. M. García Fernández, R. E. Wellinger, I. Fernández and N. Khiar, *J. Mater. Chem. B*, 2016, **4**, 2028–2037.

14 R. Recio, P. Lerena, E. Pozo, J. M. Calderón-Montaña, E. Burgos-Morón, M. López-Lázaro, V. Valdivia, M. Pernia Leal, B. Mouillac, J. Á. Organero, N. Khiar and I. Fernández, *J. Med. Chem.*, 2021, **64**, 10350–10370.

15 M. Negrete, E. Romero-Ben, A. Gutiérrez-Valencia, C. Rosales-Barrios, E. Alés, T. Mena-Barragán, J. A. Flores, M. C. Castillejos, P. De La Cruz-Ojeda, E. Navarro-Villarán, C. Cepeda-Franco, N. Khiar and J. Muntané, *ACS Appl. Bio Mater.*, 2021, **4**, 4789–4799.

16 E. Romero-Ben, T. Mena Barragán, E. García De Dionisio, E. M. Sánchez-Fernández, J. M. García Fernández, E. Guillén-Mancina, M. López-Lázaro and N. Khiar, *J. Mater. Chem. B*, 2019, **7**, 5930–5946.

17 V. Valdivia, R. Recio, P. Lerena, E. Pozo, R. Serrano, R. Calero, C. Pintado, M. P. Leal, N. Moreno-Rodríguez, J. Á. Organero, N. Khiar and I. Fernández, *Eur. J. Med. Chem.*, 2024, **15**, 116021.

18 M. Assali, J. J. Cid, M. Pernía-Leal, M. Muñoz-Bravo, I. Fernández, R. E. Wellinger and N. Khiar, *ACS Nano*, 2013, **7**, 2145–2453.

19 E. Romero-Ben, J. J. Cid, M. Assali, E. Fernández-García, R. E. Wellinger and N. Khiar, *Int. J. Nanomed.*, 2019, **14**, 3245–3263.

20 M. Assali, N. Kittana, S. Dayyeh and N. Khiar, *Nanotechnology*, 2021, **32**, 205101.

21 B. Kang, T. Opatz, K. Landfester and F. R. Wurm, *Chem. Soc. Rev.*, 2015, **44**, 8301–8325.

22 T. S. Patil and A. S. Deshpande, *J. Controlled Release*, 2020, **320**, 239–252.

23 M. Varache, S. Rizzo, E. J. Sayers, L. Newbury, A. Mason, C.-T. Liao, E. Chiron, N. Bourdiec, A. Jones, D. J. Fraser, P. R. Taylor, A. T. Jones, D. W. Thomas and E. L. Ferguson, *RSC Pharmaceutics*, 2024, **1**, 68–79.

24 M. H. Alu'datt, M. Alrosan, S. Gammoh, C. C. Tranchant, M. N. Alhamad, T. Rababah, R. Zghoul, H. Alzoubi, S. Ghatasheh, K. Ghozlan and T. C. Tan, *Food Biosci.*, 2022, **50**, 101971.

25 F. Carraro, M. J. de Velásquez-Hernández, M. Linares Moreau, E. Astria, C. Sumby, C. Doonan and P. Falcaro, in *Metal-Organic Frameworks in Biomedical and Environmental Field*, ed. P. Horcajada Cortés and S. Rojas Macías, Springer, 2021, ch. 12, pp. 379–432.

26 J. Qiu, X. Li, R. Gref and A. Vargas-Berenguel, *Metal-Organic Frameworks for Biomedical Applications*, 2020.

27 F. Demir Duman, A. Monaco, R. Foulkes, C. R. Becer and R. S. Forgan, *ACS Appl. Nano Mater.*, 2022, **5**, 13862–13873.

28 R. S. Forgan, R. A. Smaldone, J. J. Gassensmith, H. Furukawa, D. B. Cordes, Q. Li, C. E. Wilmer, Y. Y. Botros, R. Q. Snurr, A. M. Z. Slawin and J. F. Stoddart, *J. Am. Chem. Soc.*, 2012, **134**, 406–417.

29 V. Agostoni, P. Horcajada, M. Noiray, M. Malanga, A. Aykaç, L. Jicsinszky, A. Vargas-Berenguel, N. Semiramoth, S. Daoud-Mahammed, V. Nicolas, C. Martineau, F. Taulelle, J. Vigneron, A. Etcheberry, C. Serre and R. Gref, *Sci. Rep.*, 2015, **5**, 7925.

30 X. Zheng, X. Song, G. Zhu, D. Pan, H. Li, J. Hu, K. Xiao, Q. Gong, Z. Gu, K. Luo and W. Li, *Adv. Mater.*, 2024, **36**, 2308977.

31 Y. Absalan, M. Gholizadeh, E.-B. Kim, S. Ameen, Y. Wang, Y. Wang and H. He, *Coord. Chem. Rev.*, 2024, **515**, 215972.

32 A. M. de Matos, *Eur. J. Org. Chem.*, 2023, e202200919.

33 J. Lim, D. Sari-Ak and T. Bagga, *Biology*, 2021, **10**, 1178.

34 V. Cagno, E. D. Tseligka, S. T. Jones and C. Tapparel, *Viruses*, 2019, **11**, 596.

35 M. de, J. Velásquez-Hernández, M. Linares-Moreau, E. Astria, F. Carraro, M. Z. Alyami, N. M. Khashab, C. J. Sumby, C. J. Doonan and P. Falcaro, *Coord. Chem. Rev.*, 2021, **429**, 213651.

36 J. Yang and Y. W. Yang, *Small*, 2020, **16**, e1906846.

37 J. W. M. Osterrieth and D. Fairen-Jimenez, *Biotechnol. J.*, 2021, **16**, 2000005.

38 J. Tang, C. Huang, Y. Liu, T. Wang, M. Yu, H. Hao, W. Zeng, W. Huang, J. Wang and M. Wu, *Coord. Chem. Rev.*, 2023, **490**, 215211.

39 M. X. Wu and Y. W. Yang, *Adv. Mater.*, 2017, **29**, 1606134.

40 L. He, Y. Liu, J. Lau, W. Fan, Q. Li, C. Zhang, P. Huang and X. Chen, *Nanomedicine*, 2019, **14**, 1343–1365.

41 Y. Wang, J. Yan, N. Wen, H. Xiong, S. Cai, Q. He, Y. Hu, D. Peng, Z. Liu and Y. Liu, *Biomaterials*, 2020, **230**, 119619.

42 S. He, L. Wu, X. Li, H. Sun, T. Xiong, J. Liu, C. Huang, H. Xu, H. Sun, W. Chen, R. Gref and J. Zhang, *Acta Pharm. Sin. B*, 2021, **11**, 2362–2395.

43 A. Baranwal, S. A. Polash, V. K. Aralappanavar, B. K. Behera, V. Bansal and R. Shukla, *Nanomaterials*, 2024, **14**, 244.

44 Z. Sun, T. Li, T. Mei, Y. Liu, K. Wu, W. Le and Y. Hu, *J. Mater. Chem. B*, 2023, **11**, 3273–3294.

45 I. Roy and J. F. Stoddart, *Acc. Chem. Res.*, 2021, **54**, 1440–1453.

46 H. Cai, Y. L. Huang and D. Li, *Coord. Chem. Rev.*, 2019, **378**, 207–221.

47 Y. Si, H. Luo, P. Zhang, C. Zhang, J. Li, P. Jiang, W. Yuan and R. Cha, *Carbohydr. Polym.*, 2024, **323**, 121424.

48 “Saccharose” etymology: from Latin ‘saccharum,’ in turn from Greek ‘σάκχαρον’ (sakkharon), from Arabic ‘(as)sokkar,’ from Persian ‘shakar,’ from Pali ‘sakkharā,’ from Sanskrit “शर्करा” (śarkarā), meaning “sand, gravel, sugar”.

49 IUPAC, 1995, 67, 1307. Glossary of class names of organic compounds and reactivity intermediates based on structure, IUPAC Recommendations 1995, on page 1325, DOI: [10.1351/goldbook.C00820](https://doi.org/10.1351/goldbook.C00820).

50 S. J. Richards and M. I. Gibson, *JACS Au*, 2021, **1**, 2089–2099.

51 K. Kim, S. Lee, E. Jin, L. Palanikumar, J. H. Lee, J. C. Kim, J. S. Nam, B. Jana, T. H. Kwon, S. K. Kwak, W. Choe and J. H. Ryu, *ACS Appl. Mater. Interfaces*, 2019, **11**, 27512–27520.

52 H. Hamed, S. Moradi, S. M. Hudson, A. E. Tonelli and M. W. King, *Carbohydr. Polym.*, 2022, **282**, 119100.

53 Q. Xu, J. E. Torres, M. Hakim, P. M. Babiak, P. Pal, C. M. Battistoni, M. Nguyen, A. Panitch, L. Solorio and J. C. Liu, *Mater. Sci. Eng., R*, 2021, **146**, 100641.

54 T. H. Shin, P. K. Kim, S. Kang, J. Cheong, S. Kim, Y. Lim, W. Shin, J. Y. Jung, J. D. Lah, B. W. Choi and J. Cheon, *Nat. Biomed. Eng.*, 2021, **5**, 252–263.

55 K. Yang, J. Liu, L. Luo, M. Li, T. Xu and J. Zan, *RSC Adv.*, 2023, **13**, 7250–7256.

56 Y. Toomari, H. Ebrahimpour, M. Pooresmaeil and H. Namazi, *Polym. Bull.*, 2022, **80**, 4407–4428.

57 M. B. Mukherjee, R. Mullick, B. U. Reddy, S. Das and A. M. Raichur, *ACS Appl. Bio Mater.*, 2020, **3**, 7598–7610.

58 J. D. Xiao, R. Li and H. L. Jiang, *Small Methods*, 2023, **7**, 2300702.

59 A. Zuliani, N. Khiar and C. Carrillo-Carrión, *Anal. Bioanal. Chem.*, 2023, **415**, 2005–2023.

60 S. F. A. Rizvi, H. Zhang and Q. Fang, *Med. Res. Rev.*, 2024, **44**, 2420–2471.

61 A. Zhang, K. Meng, Y. Liu, Y. Pan, W. Qu, D. Chen and S. Xie, *Adv. Colloid Interface Sci.*, 2020, **284**, 102261.

62 L. Guerrini, R. A. Alvarez-Puebla and N. Pazos-Perez, *Materials*, 2018, **11**, 1154.

63 L. Wang, Z. Li, Y. Wang, M. Gao, T. He, Y. Zhan and Z. Li, *Nanoscale*, 2023, **15**, 10529–10557.

64 L. Meng, J. Ren, Z. Liu and Y. Zhao, *J. Drug Delivery Sci. Technol.*, 2022, **70**, 103193.

65 Z. Cai, F. Xin, Z. Wei, M. Wu, X. Lin, X. Du, G. Chen, D. Zhang, Z. Zhang, X. Liu and C. Yao, *Adv. Healthcare Mater.*, 2019, **9**, 1900996.

66 W. Cai, H. Gao, C. Chu, X. Wang, J. Wang, P. Zhang, G. Lin, W. Li, G. Liu and X. Chen, *ACS Appl. Mater. Interfaces*, 2017, **9**, 2040–2051.

67 X. Fu, Z. Yang, T. Deng, J. Chen, Y. Wen, X. Fu, L. Zhou, C. Yu and Z. Zhu, *J. Mater. Chem. B*, 2020, **8**, 1481–1488.

68 N. Song, B. Li, D. Li and Y. Yan, *APL Mater.*, 2023, **11**, 081112.

69 X. Xu, Y. Chen, Y. Zhang, Y. Yao and P. Ji, *J. Mater. Chem. B*, 2020, **8**, 9129–9138.

70 F. Shu, D. Lv, X. L. Song, B. Huang, C. Wang, Y. Yu and S. C. Zhao, *RSC Adv.*, 2018, **8**, 6581–6589.

71 V. V. Vinogradov, A. S. Drozdov, L. R. Mingabudinova, E. M. Shabanova, N. O. Kolchina, E. I. Anastasova, A. A. Markova, A. A. Shtil, V. A. Milichko, G. L. Starova, R. L. M. Precker, A. V. Vinogradov, E. Hey-Hawkins and E. A. Pidko, *J. Mater. Chem. B*, 2018, **6**, 2450–2459.

72 H. Zhang, Y. Shang, Y. H. Li, S. K. Sun and X. B. Yin, *ACS Appl. Mater. Interfaces*, 2018, **11**, 1886–1895.

73 V. R. Cherkasov, E. N. Mochalova, A. V. Babenyshev, J. M. Rozenberg, I. L. Sokolov and M. P. Nikitin, *Acta Biomater.*, 2020, **103**, 223–236.

74 S. Javanbakht, M. Pooresmaeil, H. Hashemi and H. Namazi, *Int. J. Biol. Macromol.*, 2018, **119**, 588–596.

75 M. Parsaei and K. Akhbari, *Inorg. Chem.*, 2022, **61**, 19354–19368.

76 N. Jin, B. Wang, X. Liu, C. Yin, X. Li, Z. Wang, X. Chen, Y. Liu, W. Bu and H. Sun, *J. Nanobiotechnol.*, 2023, **21**, 426.

77 W. Chen, M. Yang, H. Wang, J. Song, C. Mei, L. Qiu and J. Chen, *Adv. Healthcare Mater.*, 2024, **13**, 2304000.

78 S. Das, P. Kudale, P. Dandekar and P. V. Devarajan, in *Targeted Intracellular Drug Delivery by Receptor Mediated Endocytosis*, ed. P. V. Devarajan, P. Dandekar and A. A. D’Souza, Springer International Publishing, Berlin, 2019.

79 A. U. Ortiz, A. P. Freitas, A. Boutin, A. H. Fuchs and F. X. Coudert, *Phys. Chem. Chem. Phys.*, 2014, **16**, 9940–9949.

80 R. E. Giménez, E. Piccinini, O. Azzaroni and M. Rafti, *ACS Omega*, 2019, **4**, 842–848.

81 M. Moradi, M. Aliomrani, S. Tangestaninejad, J. Varshosaz, H. Kazemian, F. S. Emami and M. Rostami, *Appl. Organomet. Chem.*, 2022, **36**, e6755.

82 A. Abednejad, A. Ghaei, J. Nourmohammadi and A. A. Mehrizi, *Carbohydr. Polym.*, 2019, **222**, 115033.

83 E. Bellido, T. Hidalgo, M. V. Lozano, M. Guillevic, R. Simón-Vázquez, M. J. Santander-Ortega, Á. González-Fernández, C. Serre, M. J. Alonso and P. Horcajada, *Adv. Healthcare Mater.*, 2015, **4**, 1246–1257.

84 D. Bhatt, S. Singh, N. Singhal, N. Bhardwaj and A. Deep, *Anal. Bioanal. Chem.*, 2023, **415**, 659–667.

85 W. Ma, B. Yang, J. Li, M. Liu, X. Li and H. Liu, *Microchim. Acta*, 2022, **189**, 253.

86 J. Cui, C. Zhang, H. Liu, L. Yang, X. Liu, J. Zhang, Y. Zhou, J. Zhang and X. Yan, *ACS Appl. Mater. Interfaces*, 2023, **15**, 11520–11535.

87 J. Hu, W. Wu, Y. Qin, C. Liu, P. Wei, J. Hu, P. H. Seeberger and J. Yin, *Adv. Funct. Mater.*, 2020, **30**, 1910084.

88 W. Cao, S. Xie, Y. Liu, P. Ran, Z. Zhang, Q. Fang and X. Li, *Adv. Funct. Mater.*, 2024, **34**, 2312866.

89 A. N. Nikam, A. Pandey, S. H. Nannuri, G. Fernandes, S. Kulkarni, B. S. Padya, S. Birangal, G. G. Shenoy, S. D. George and S. Mutualik, *Crystals*, 2022, **12**, 1484.

90 Y. Shao, H. Suo, S. Wang, Y. Peng, X. Chu, Z. Long, K. Du, L. Su, X. Sun, X. Wang, Q. Wang, R. Li and B. Wang, *Chem. Eng. J.*, 2024, **481**, 148576.

91 X. Hu, R. Li, J. Liu, K. Fang, C. Dong and S. Shi, *Adv. Healthcare Mater.*, 2024, **13**, 2302333.

92 Q. Zhou, D. Xie, K. Wang, F. Wang, Q. Wang, Y. Huang, M. Yu, J. Huang and Y. Zhao, *Drug Delivery Transl. Res.*, 2024, DOI: [10.1007/s13346-024-01652-4](https://doi.org/10.1007/s13346-024-01652-4).

93 S. Kulkarni, A. Pandey, S. Soman, S. H. Nannuri, A. Kumar, D. Bhavsar, S. D. George, S. Subramanian and S. Mutualik, *Int. J. Biol. Macromol.*, 2024, **278**, 134381.

94 Z. Li, S. He, L. Xie, G. Zeng, J. Huang, H. Wang, H. Chen, T. Deng, Y. Xia, C. Huang and Z. Chen, *Adv. Funct. Mater.*, 2024, 2411247, DOI: [10.1002/adfm.202411247](https://doi.org/10.1002/adfm.202411247).

95 X. Lu, X. Yu, B. Li, X. Sun, L. Cheng, Y. Kai, H. Zhou, Y. Tian and D. Li, *Adv. Sci.*, 2024, 2405643, DOI: [10.1002/advs.202405643](https://doi.org/10.1002/advs.202405643).

96 H. Li, C. Zhang, Y. Chen, Y. Xu, W. Yao and W. Fan, *ACS Nano*, 2024, **18**, 23711–23726.

97 Y. Lou, Z. Wang and Y. Wang, *Colloids Surf. A*, 2024, **703**, 135217.

98 Q. An, Z. Dai, J. Zhang, H. Hu, J. Wang, X. Cao, Z. Hu, Y. Sun, L. Tian and X. Zheng, *ACS Appl. Nano Mater.*, 2024, **7**, 11757–11766.

99 X. Wan, Y. Zhang, T. Zheng, W. Pan, W. Zhu, N. Li and B. Tang, *Mater. Today Nano*, 2024, **26**, 100484.

100 X. Sun, H. Li, L. Qi, F. Wang, Y. Hou, J. Li and S. Guan, *Prog. Org. Coat.*, 2024, **187**, 108177.

101 A. R. Ahangarkolaei, A. Binaeian, A. H. Kasgari, P. Valipour and E. Binaeian, *J. Porous Mater.*, 2024, **31**, 2193–2203.

102 Q. Sun, T. Yuan, G. Yang, D. Guo, L. Sha and R. Yang, *Int. J. Biol. Macromol.*, 2023, **253**, 127519.

103 C. R. Quijia, A. Ocaña, C. Alonso-Moreno, R. C. Galvão Frem and M. Chorilli, *J. Mol. Struct.*, 2024, **1305**, 137801.

104 A. Taghikhani, M. Babazadeh, S. Davaran and E. Ghasemi, *Colloids Surf. B*, 2024, **243**, 114122.

105 M. Dousti, A. Golmohamadpour, Z. Hami and Z. Jamalpoor, *Nanotechnology*, 2024, **35**, 145101.

106 S. Zhang, H. Liu, D. Fu, H. Zhao, D. Zhang and T. Lü, *J. Chromatogr. A*, 2024, **1735**, 465347.

107 X. Mao, Y. Lu, X. Zhang and Y. Huang, *Talanta*, 2018, **188**, 161–167.

108 M. Pooresmaeil and H. Namazi, *Int. J. Pharm.*, 2022, **625**, 122112.

109 A. Guo, M. Durymanov, A. Permyakova, S. Sene, C. Serre and J. Reineke, *Pharm. Res.*, 2019, **36**, 53.

110 B. Gao, K. Yang, M. Yang, W. Li, T. Jiang, R. Gao, Y. Pei, Z. Pei and Y. Lv, *Chem. Commun.*, 2024, **60**, 8892–8895.

111 P. H. Tong, L. Zhu, Y. Zang, J. Li, X. P. He and T. D. James, *Chem. Commun.*, 2021, **57**, 12098–12110.

112 M. D. J. Velásquez-Hernández, E. Astria, S. Winkler, W. Liang, H. Wiltsche, A. Poddar, R. Shukla, G. Prestwich, J. Paderi, P. Salcedo-Abraira, H. Amenitsch, P. Horcajada, C. J. Doonan and P. Falcaro, *Chem. Sci.*, 2020, **11**, 10835–10843.

113 E. Astria, M. Thonhofer, R. Ricco, W. Liang, A. Chemelli, A. Tarzia, K. Alt, C. E. Hagemeyer, J. Rattenberger, H. Schroettner, T. Wrodnigg, H. Amenitsch, D. M. Huang, C. J. Doonan and P. Falcaro, *Mater. Horiz.*, 2019, **6**, 969–977.

114 N. Hammı, S. El Hankari, N. Katir, N. Marcotte, K. Draoui, S. Royer and A. El Kadib, *Microporous Mesoporous Mater.*, 2020, **306**, 110429.

115 P. Raju, K. Balakrishnan, M. Mishra, T. Ramasamy and S. Natarajan, *J. Drug Delivery Sci. Technol.*, 2022, **70**, 103223.

116 R. Zhao, T. Chen, Y. Li, L. Chen, Y. Xu, X. Chi, S. Yu, W. Wang, D. Liu, B. Zhu and J. Hu, *Food Chem.*, 2024, **448**, 139167.

117 Y. Liu, C. Yuan, B. Cui, M. Zhao, B. Yu, L. Guo, P. Liu and Y. Fang, *Food Chem.*, 2024, **443**, 138543.

118 A. Cioci, P. Benzi, C. Canepa, L. Mortati, A. de la Paz, I. M. Garnica-Palafox, F. M. Sánchez-Arévalo, R. C. Dante and D. Marabello, *Inorganics*, 2024, **12**, 231.

119 R. Zhao, T. Chen, Y. Li, L. Chen, Y. Xu, X. Chi, S. Yu, W. Wang, D. Liu, B. Zhu and J. Hu, *Food Chem.*, 2024, **448**, 139167; D. Marabello, P. Antoniotti, P. Benzi, C. Canepa, E. Diana, L. Operi, L. Mortati and M. P. Sassi, *J. Mater. Sci.*, 2015, **50**, 4330–4341.

120 Y. Liu, C. Yuan, B. Cui, M. Zhao, B. Yu, L. Guo, P. Liu and Y. Fang, *Food Chem.*, 2024, **443**, 138543; D. Marabello, P. Antoniotti, P. Benzi, C. Canepa, L. Mortati and M. P. Sassi, *Acta Crystallogr., Sect. B: Struct. Sci., Cryst. Eng. Mater.*, 2017, **73**, 737–743.

121 B. P. Carpenter, A. R. Talosig, B. Rose, G. Di Palma and J. P. Patterson, *Chem. Soc. Rev.*, 2023, **52**, 6918–6937.

122 Y. Xu, Y. Liu, H. Han and Z. Ma, *Chem. Mater.*, 2022, **34**, 4242–4247.

123 Z. Meng, B. Yu, Y. Chen, Y. Deng, H. Li, J. Yao and H. Y. Yang, *Chem. Eng. Sci.*, 2024, **284**, 119527.

124 T. De Villenoisy, N. Ho, S. Chen, X. Zheng, C. C. Sorrell, Y. Zhang and P. Koshy, *Mater. Chem. Phys.*, 2023, **309**, 128448.

125 C. M. Cova, L. Boffa, M. Pistocchi, S. Giorgini, R. Luque and G. Cravotto, *Molecules*, 2019, **24**, 2681.

126 A. Zuliani, M. Cano, F. Calsolaro, A. R. Puente Santiago, J. J. Giner-Casares, E. Rodríguez-Castellón, G. Berlier, G. Cravotto, K. Martina and R. Luque, *Sustainable Energy Fuels*, 2021, **5**, 720–731.

127 A. Zuliani, S. Chen and R. Giorgi, *Appl. Mater. Today*, 2023, **30**, 101716.

128 A. Zuliani, D. Bandelli, D. Chelazzi, R. Giorgi and P. Baglioni, *J. Colloid Interface Sci.*, 2022, **614**, 451–459.

129 C. M. Cova, A. Zuliani, R. Manno, V. Sebastian and R. Luque, *Green Chem.*, 2020, **22**, 1414–1423.

130 M. Chang, C. Tang, C. C. Wang and C. Zhao, *Prog. Nat. Sci.: Mater. Int.*, 2024, **34**, 66–73.

131 H. Ding, Q. Xia, J. Shen, C. Zhu, Y. Zhang and N. Feng, *Colloids. Surf. B Biointerfaces*, 2023, **232**, 113607.



132 C. M. Cova, V. Ramos, A. Escudero, J. P. Holgado, N. Khiar and A. Zuliani, *Green Chem.*, 2024, DOI: [10.1039/D4GC03743J](https://doi.org/10.1039/D4GC03743J).

133 A. Bandyopadhyay, T. Das, S. Nandy, S. Sahib, S. Preetam, A. V. Gopalakrishnan and A. Dey, *Naunyn-Schmiedebergs Arch.*, 2023, **396**, 3417–3441.

134 M. A. Rahim, N. Jan, S. Khan, H. Shah, A. Madni, A. Khan, A. Jabar, S. Khan, A. Elhissi, Z. Hussain, H. C. Aziz, M. Sohail, M. Khan and H. E. Thu, *Cancers*, 2021, **13**, 6710.

135 R. S. Forgan, *Commun. Mater.*, 2024, **5**, 46.